

35933



National Library of Canada

Bibliothèque nationale du Canada

CANADIAN THESES ON MICROFICHE

THÈSES CANADIENNES SUR MICROFICHE

NAME OF AUTHOR/NOM DE L'AUTEUR Josef LANDA

TITLE OF THESIS/TITRE DE LA THÈSE Liquid-Solid Type Phase Transition of Benzene Adsorbed on Charcoal, Silica Gel and Cab-O-Sil.

UNIVERSITY/UNIVERSITÉ Simon Fraser University

DÉGREE FOR WHICH THESIS WAS PRESENTED /
GRADE POUR LEQUEL CETTE THÈSE FUT PRÉSENTÉE Master of Science

YEAR THIS DEGREE CONFERRED/ANNÉE D'OBTENTION DE CE GRADE 1976

NAME OF SUPERVISOR/NOM DU DIRECTEUR DE THÈSE E.J. Wells

Permission is hereby granted to the NATIONAL LIBRARY OF CANADA to microfilm this thesis and to lend or sell copies of the film.

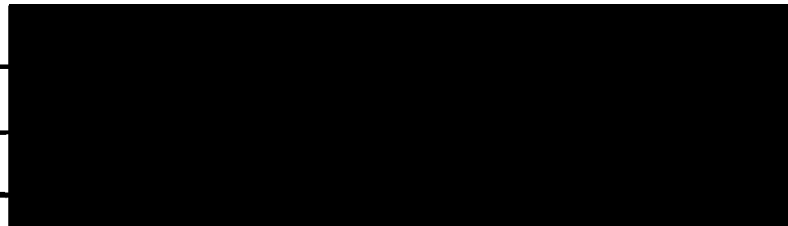
L'autorisation est, par la présente, accordée à la BIBLIOTHÈQUE NATIONALE DU CANADA de microfilmer cette thèse et de prêter ou de vendre des exemplaires du film.

The author reserves other publication rights, and neither the thesis nor extensive extracts from it may be printed or otherwise reproduced without the author's written permission.

L'auteur se réserve les autres droits de publication; ni la thèse ni de longs extraits de celle-ci ne doivent être imprimés ou autrement reproduits sans l'autorisation écrite de l'auteur.

DATED/DATE Apr 21, 1976 SIGNED/SIGNÉ _____

PERMANENT ADDRESS/RÉSIDENCE FIXE _____





National Library of Canada

Cataloguing Branch
Canadian Theses Division

Ottawa, Canada
K1A 0N4

Bibliothèque nationale du Canada

Direction du catalogage
Division des thèses canadiennes

NOTICE

The quality of this microfiche is heavily dependent upon the quality of the original thesis submitted for microfilming. Every effort has been made to ensure the highest quality of reproduction possible.

If pages are missing, contact the university which granted the degree.

Some pages may have indistinct print especially if the original pages were typed with a poor typewriter ribbon or if the university sent us a poor photocopy.

Previously copyrighted materials (journal articles, published tests, etc.) are not filmed.

Reproduction in full or in part of this film is governed by the Canadian Copyright Act, R.S.C. 1970, c. C-30. Please read the authorization forms which accompany this thesis.

**THIS DISSERTATION
HAS BEEN MICROFILMED
EXACTLY AS RECEIVED**

AVIS

La qualité de cette microfiche dépend grandement de la qualité de la thèse soumise au microfilmage. Nous avons tout fait pour assurer une qualité supérieure de reproduction.

S'il manque des pages, veuillez communiquer avec l'université qui a conféré le grade.

La qualité d'impression de certaines pages peut laisser à désirer, surtout si les pages originales ont été dactylographiées à l'aide d'un ruban usé ou si l'université nous a fait parvenir une photocopie de mauvaise qualité.

Les documents qui font déjà l'objet d'un droit d'auteur (articles de revue, examens publiés, etc.) ne sont pas microfilmés.

La reproduction, même partielle, de ce microfilm est soumise à la Loi canadienne sur le droit d'auteur, SRC 1970, c. C-30. Veuillez prendre connaissance des formules d'autorisation qui accompagnent cette thèse.

**LA THÈSE A ÉTÉ
MICROFILMÉE TELLE QUE
NOUS L'AVONS REÇUE**

LIQUID-SOLID TYPE PHASE TRANSITION OF BENZENE ADSORBED ON
CHARCOAL, SILICA GEL AND CAB-O-SIL

by

Josef Landa

M.Sc., Technical University of Prague

A THESIS SUBMITTED IN PARTIAL FULFILLMENT OF

THE REQUIREMENTS FOR THE DEGREE OF

MASTER OF SCIENCE

in the Department

of

Chemistry



Josef Landa, 1976

SIMON FRASER UNIVERSITY

January 1976

All rights reserved. This thesis may not be
reproduced in whole or in part, by photocopy
or other means, without permission of the author.

APPROVAL

Name: Josef Landa
Degree: Master of Science
Title of Thesis: Liquid-Solid Type Phase Transition
of Benzene Adsorbed on Charcoal,
Silica Gel and Cab-O-Sil.

Examining Committee:

Chairman: R.J. Cushley

E.S. Wells, Senior Supervisor

L.K. Peterson

J. Walkley

D. Crozier

Date Approved: 21 Apr 76

PARTIAL COPYRIGHT LICENSE

I hereby grant to Simon Fraser University the right to lend my thesis or dissertation (the title of which is shown below) to users of the Simon Fraser University Library, and to make partial or single copies only for such users, or in response to a request from the library of any other university, or other educational institution, on its own behalf or for one of its users. I further agree that permission for multiple copying of this thesis for scholarly purposes may be granted by me or the Dean of Graduate Studies. It is understood that copying or publication of this thesis for financial gain shall not be allowed without my written permission.

Title of Thesis/Dissertation:

Liquid-Solid Type Phase Transition of Benzene Adsorbed on
Charcoal, Silica Gel and Cab-O-Sil

Author: _____

(signature)

Josef LANDA

(name)

April 21, 1976
(date)

A B S T R A C T

The proton CW NMR spectra of benzene adsorbed on charcoal, silica gel and Cab-o-sil have been measured at various temperatures in the range 30 °C to -100 °C. Sudden changes in the temperature dependence of the NMR signal intensities evaluated from the spectra are interpreted as a liquid-solid phase transition. A discussion of the suitability of the NMR signal intensities as a measure of relative contents of phases is given.

Differential scanning calorimetry measurements made on the same adsorption systems show thermal effects at approximately the same temperatures and thus confirm that the phase transition is of the first order.

It has been found that the phase transition of adsorbed benzene on all the adsorbents studied occurs at temperatures lower than the normal melting point of benzene and that the amounts of phases change gradually over a certain temperature range during the transition.

C O N T E N T S

	page
1. Introduction	1
2. Phase content determination by NMR	4
3. Experimental	9
3.1. Materials	9
3.1.1. Adsorbents	9
3.1.2. Adsorbate	9
3.1.3. Adsorbents characteristics	10
3.2. NMR measurements	11
3.2.1. Apparatus	11
3.2.2. Preparation of NMR samples	12
3.2.3. Spectra measurements	12
3.3. Differential scanning calorimetry	14
3.3.1. Preparation of samples	14
3.3.2. Measurements	15
4. Results and interpretation	16
4.1. NMR measurements	16
4.1.1. System benzene / charcoal	18
4.1.2. System benzene / silica gel	18
4.1.3. System benzene / Cab-o-sil	34
4.2. DSC measurements	41
4.2.1. System benzene / charcoal	41
4.2.2. System benzene / silica gel	46
4.2.3. System benzene / Cab-o-sil	49
5. Discussions	50
References	56

1. Introduction

When a substance is adsorbed on a solid surface, certain of its physical properties are modified, sometimes to a very considerable degree. It seems to be definitely established that the melting points of adsorbed substances on porous adsorbents are lower than those of the corresponding bulk substances (1).

The phenomenon, besides its basic importance in adsorption theory, could play an important part in heterogenous nucleation theory and has considerable technical and economic importance in connection with the liquid-solid phase transition of water contained in capillary systems such as soil and building materials.

The frost action, freezing and thawing of soil and their resulting effects on contacting materials and structures, and a related effect called frost heaving, the raising of ground surface due to the formation of ice in the underlying soil, are both complicated phenomena, not fully understood, and have considerable importance in construction engineering as a possible cause of damage of ground surface structures such as highways, airfield pavements, and canals (2). Freezing of adsorbed water is also important in building materials technology (3), hydrology (2), and it was studied in connection with hail formation and its prevention (4).

The liquid-solid type transitions of adsorbates have been studied by a number of techniques, such as measurements of adsorption isosteres (5,6,7), measurements of heat capacities (8,9,7,10,11,12), dilatometric measurements (13,14,15,16,17), measurements of dielectric constants (18,19), NMR spectroscopy

(21,22,23), and X-ray diffraction (29). However, reliable data covering more aspects of the phenomena are scarce, partly due to the difficulties in attaining an equilibrium state in the region of the phase transition and due to extensive experimental measurements needed. Reviews on the subject may be found in the excellent monographs of Brunauer (1), Young and Crowell (24), and a review article of Dubinin (25).

The general picture which may be drawn from reported data is that on the systems with porous adsorbents, such as silica gel (6,8,12,18,20) and ferric oxide gel (5), the melting point of adsorbate is lower than in the bulk phase and the melting is not sharp, but occurs in a certain interval of temperatures. From experimental data accumulated until now, no conclusion about specific interactions between adsorbent and adsorbate concerning the liquid-solid transition can be drawn.

The lowering of the melting points in capillary systems is explained on the basis of the capillary condensation theory as a consequence of the equilibrium between the solid adsorbate, present in normal bulk form, and capillary liquid, having lower vapor tension than bulk liquid at the same temperature (5,12,19).

Rather surprising results of calorimetric measurements were reported by Morricon et al. (7,9) showing, that in the systems nitrogen and argon adsorbed on rutile which can be considered as a non-porous adsorbent, similar phase transitions occur and also, that the vapour pressure in melting region was lower than the vapour pressure of the corresponding bulk solid. It seems unlikely that in these systems the capillary condensation can play any important part,

and also the assumption of the presence of the bulk solid adsorbate is not compatible with experimentally found vapour pressures.

In this work the solid liquid type transition of adsorbed benzene was studied on three adsorbents of different porosity, using magnetic resonance absorption for determination of relative amounts of phases. The object was to determine if the liquid-solid type of transition can be detected, particularly on Cab-o-sil, which may be considered as a non-porous adsorbent.

Comparison with differential scanning calorimetry measurements was made to determine if the phase transition is of the first order, partly due to the possibility, pointed out by Resing (34), of an "apparent" non-thermodynamic transition, which may be an artefact of the NMR technique.

On the next pages, in Section 2, the suitability of the NMR technique for determination of relative amounts of phases in multi-phase systems is discussed.

In Section 3, there are described experimental procedures of preparation of samples, and NMR and DSC measurements.

Results are summarized and discussed in Sections 4 and 5.

2. Phase content determination by NMR

NMR technique offers, in principle at least, a suitable means of observing phase transitions in adsorbed layers. In comparison with some other methods, for instance methods based on analysis of adsorption data, where only the onset of the formation of the new phase is detected, the NMR method has also the advantage that it may determine the relative contents of phases in multiphase systems.

The underlying principles are that the signal intensity is proportional to the number of magnetic nuclei and that the molecules in different states of aggregation have different mobilities and different local magnetic fields.

The use of NMR as a tool of quantitative analysis has been reviewed by several authors (30,31,32). The dependence of the signal intensity on some of the instrumental factors was discussed by Williams (33), who pointed out, that for accurate intensity measurements, the problems of magnetic field and r.f. transmitter instabilities, nonlinearities associated with the resonance signal in the receiver and the recorder have to be overcome. These factors are mainly design problems of apparatus. Because of the dependence of the signal intensity on the instrumental factors such as the Q of the sample circuit, effective volume of the coil, filling factor, receiver pass band width, which cannot be evaluated precisely, only relative measurements with respect to some standard are possible.

Apart from the instrumentation problems, the main problem in quantitative analysis by NMR arises from the dependence of the

absorption on the values of T_1 , T_2 and H_1 as can be seen from the equations (1) and (1a), which were obtained by combining the Faraday law with solutions of Bloch equations for steady state conditions

(30).

$$V_V \propto \omega \chi_0 H_0 \gamma H_1 T_2 / (1 + T_2^2 (\omega_0 - \omega)^2 + s) \quad (1)$$

and

$$V_U \propto \omega \chi_0 H_0 \gamma H_1 T_2 (\omega_0 - \omega) / (1 + T_2^2 (\omega_0 - \omega)^2 + s) \quad (1a)$$

where V_V and V_U are the voltages induced in the receiver coil for the absorption and the dispersion made respectively, ω and ω_0 are frequency and resonance frequency respectively, T_1 and T_2 are the longitudinal and the transverse relaxation times, H_1 and H_0 are the r.f. and the constant magnetic fields respectively, χ_0 is magnetic susceptibility, and s is the saturation factor defined as

$$s = \gamma^2 H_1^2 T_1 T_2 \quad (2)$$

The magnetic susceptibility is related to the number of nuclei N in unit volume, and consequently to the concentration of studied substance in the effective volume of the receiver coil, by the equation

$$\chi_0 = (l(l+1)\mu^2 / 3kT)N \quad (3)$$

where μ is the magnetic moment of the nuclei, l is the spin number and k is the Boltzman constant.

The quantities related to the concentration of the nuclei studied, which may be evaluated from the absorption made spectra are maximum intensity or peak height $V_{V,max}$ and the area under the curve signal intensity vs frequency, i.e. integral I_V of $V_V(\omega)$ in the interval $\omega \in (0, \infty)$. From equation (1), we find

$$V_{V,max} \propto \chi_0 H_1 T_2 / (1+s) \quad (4)$$

and

$$I_v \propto \chi_0 H_1 / (1+s)^{\frac{1}{2}} \quad (5)$$

By comparison of the equations (4) and (5) it is apparent that for low r.f. fields, where $s \ll 1$, the peak heights are dependent on T_2 and therefore usable only if the lines are of identical width, whereas the integrated intensities are independent of T_2 .

The use of the integrated intensities is preferable even at higher r.f. fields where the saturation factor is not negligible, because the linear dependence on concentration is less influenced and their values tend to finite limits as H_1 tends to infinity, whereas the peak heights tend to zero.

There are some advantages in using the dispersion mode signal for intensity evaluation. As can be seen from equation (1a) $V_u(\omega)$ is an odd function and has local extrema at

$$\omega_0 - \omega = \pm (1/T_2)(1+s)^{\frac{1}{2}} \quad (6)$$

where the signal intensity is

$$V_{u,extr} \propto \pm \chi_0 H_1 T_2 / (1+s)^{\frac{1}{2}} \quad (7)$$

The integral of $V_u(\omega)$ in the interval $\omega \in (\omega_0, \infty)$ is divergent, but a useful expression can be obtained by integration in the interval $(\omega_0, \omega_0 + (1/T_2)(1+s)^{\frac{1}{2}})$

$$I_{u,extr} \propto \chi_0 H_1 \quad (8)$$

As can be seen, the resulting integral is independent of both relaxation times T_1 and T_2 .

The dependence of signal intensities on temperature is determined by temperature dependence of instrumental factors, and by temperature dependence of magnetic susceptibility given by equation (3). Minimization of temperature dependence of instrumental factors is a

design problem. The dependence of magnetic susceptibility on temperature may be taken into account by using the Curie law.

The quantitative determination of the amounts of phases in a two-phase system can be based on the fact that the mobility of nuclei in one phase is much less than in the other; as a consequence, the resonance spectrum of such a system consists of a relatively narrow line arising from the nuclei of more mobile phase superimposed on a broad line of nuclei in less mobile phase. The implicit assumption here is that there is no exchange of nuclei between the phases, or it is so slow, in comparison with relaxation times, that each phase behaves as if it were isolated from the other.

If we have two phases α and β , without any exchange involved and with the same resonance frequency, then the resulting signal V_{t} is a superposition of the signals of the individual phases V^{α} , V^{β} .

For the absorption mode signal the total peak height is

$$V_{\text{max,t}} = V_{\text{max}}^{\alpha} + V_{\text{max}}^{\beta} \quad (9)$$

$$N^{\alpha} T_2^{\alpha} / (1+s^{\alpha}) + N^{\beta} T_2^{\beta} / (1+s^{\beta})$$

and the relative error in intensity made, if we read $V_{\text{max,t}}$ instead of V_{max}^{α} , is

$$\delta_{\text{rel}} = (N^{\beta} T_2^{\beta}) / (N^{\alpha} T_2^{\alpha}) \cdot (1+s^{\alpha}) / (1+s^{\beta}) \quad (10)$$

This is valid, if the heights are read relatively to the "true baseline", i.e. line defined by $V_{\text{v}} = 0$. In practise, because only part of the spectrum is recorded, the baseline is taken as a straight line passing through some points $V_{\text{B}}(\omega_{\text{B}})$, $V_{\text{B}}(\omega_0 - \omega_{\text{B}})$. In this case relative error in intensity is

$$\delta'_{rel} = \delta_{rel} - \frac{N^a T_2^a}{(1+(T_2^a)^2(\omega_0-\omega_B)^2 + s^a)} + \frac{N^B T_2^B}{(1+(T_2^B)^2(\omega_0-\omega_B)^2 + s^B)} (1+s^a) / (N^a T_2^a) \quad (11)$$

Similarly for the integrated intensity, if it is integrated in the interval $\omega \in (\omega_B, \omega_0 - \omega_B)$ and the baseline is taken as a straight line passing through points $V_B(\omega_B)$, $V_B(\omega_0 - \omega_B)$, the relative error is given by

$$\begin{aligned} \delta''_{rel} = & (2/\pi) (\arctan(T_2^a(\omega_0-\omega_B)/(1+s^a)^{1/2}) \\ & + (N^B/N^a) \arctan(T_2^B(\omega_0-\omega_B)/(1+s^B)^{1/2}) \\ & - T_2^a(\omega_0-\omega_B)(1+s^a) / (1+(T_2^a)^2(\omega_0-\omega_B)^2 + s^a) \\ & - (N^B/N^a) T_2^B(\omega_0-\omega_B) (1+s^a) / (1+(T_2^B)^2(\omega_0-\omega_B)^2 + s^B)) \\ & - 1 \end{aligned} \quad (12)$$

It should be stressed that the above considerations are valid only for Lorentzian shaped lines, however, they may serve as a guidelines in general.

In the case of benzene, the width of lines at maximum slope values are 2.80 gauss at 273°K and 2.82 gauss at 180°K (35). If the line width at half-maximum intensity of adsorbed benzene were 250 Hz and the sweep width of the spectrum 5000 Hz, then the expected error would be about 6% of the true value of the mobile phase amount, for the ratio of phase amounts 1:1.

However, if relative measurements are made by comparing the values of integrals, then the error will be smaller.

3. Experimental

3.1. Materials

3.1.1. Adsorbents

Adsorbents used in this study were:

Charcoal, activated, "Darco" G-60, 20-40 mesh from Matheson Coleman & Bell Co., Norwood, Ohio;

Silica gel, "For gas chromatography", 60-80 mesh from the same company, and

a type of aerogel silica, Cab-o-sil, grade M-7D, from Cabot Corporation, Boston, Massachusetts.

All adsorbents were first dried in vacuum at 200 °C and then extracted with benzene in a Soxhlet apparatus for approximately 170 hours to remove possibly present benzene soluble compounds. In the case of the charcoal the extraction was prolonged to approximately 500 hours. The samples were then dried in vacuum at 100 °C and used for all NMR, adsorption, and DSC measurements.

3.1.2. Adsorbate

The adsorbate used was benzene, B-411, Spectranalyzed, with certified freezing point 5.2 °C, from Fischer Scientific Co., Fair

Lawn, New Jersey. It was dried over metallic sodium and kept over sodium in a reservoir attached to the adsorption apparatus. Before admitting to the adsorbent, the benzene was degassed by repeated distillation in vacuum.

3.1.3. Adsorbents Characteristics

Adsorption isotherms of nitrogen were measured for all three adsorbents at the temperature of boiling liquid nitrogen using the gravimetric method. The adsorbent samples were treated in the same way as the samples used for the NMR measurements. The employed adsorption apparatus consisted of a Worden microbalance, with magnetic compensation, of sensitivity $2 \mu\text{g}$ and a mercury U-manometer and two McLeod gauges. BET specific surface areas were evaluated from measured data and are given in Table I. The molecular area of nitrogen was taken as 16.2 \AA^2 .

Table I.

Adsorbent	Surface area m^2/g
Charcoal	682
Silica gel	697
Cab-o-sil	180

3.2. NMR Measurements

3.2.1. Apparatus

Nuclear magnetic studies were performed on the Varian Model XL-100 spectrometer. The standard Varian Model V-4415 probe unit with the gas-flow type temperature control was used, with insert for 12mm sample tubes. The cooling medium was nitrogen gas passed through a heat exchanger filled with liquid nitrogen.

The NMR sample tube itself was equipped with a high vacuum stopcock (Ace Glass Inc., type 8195) and provided with a thermocouple well, to allow measurements of temperature in situ, to make possible NMR studies on the same sample of adsorbent with different adsorbate coverages, and to permit determination of the free volume of the NMR sample tube. The tube could be easily attached and detached via a Cajon Ultra-Torr fitting to the manifold of a high vacuum adsorption apparatus without changing the adsorbate amount in the tube. To minimize temperature gradient in the sample along the longitudinal axis of the tube and the subsequent redistribution of adsorbate due to temperature differences, a thin-walled (~0.4mm) tube was used and the amount of adsorbent was kept as small as possible. The standard adsorbent column height used was about 17mm.

The temperature of the sample was measured by means of the copper-constantan thermocouple junction inserted in the well of the NMR sample tube. The reference junction was kept at the temperature of an ice-water bath.

Care was taken to keep temperature - time dependence monotonic, to avoid an interference of possible hysteresis.

3.2.2. Preparation of NMR samples

The NMR sample tube with an adsorbent was attached to the adsorption apparatus and the adsorbent was degassed at 350 °C for 48 hours after the residual pressure was $<5 \times 10^{-6}$ torr. The sample tube with degassed adsorbent was then weighed on the analytical balance to determine the weight of the adsorbent. The tube was again attached to the adsorption apparatus and the required amount of benzene vapor was adsorbed, keeping the end of the sample tube with adsorbent in ice-water bath. A mercury U-manometer was used to measure equilibrium pressure. However, the amount of adsorbate in the sample tube was determined by direct weighing of the sample tube after it was detached.

This procedure was repeated with each NMR sample; except after the first adsorption of benzene vapor the sample was degassed at room temperature for 2 hours.

3.2.3. Spectra Measurements

Using the spectrometer in frequency-sweep mode, proton spectra were recorded for each adsorbent sample and coverage at various temperatures. Starting with the apparatus steady state temperature the temperature was decreased approximately at the rate 0.25 °C/min. to the next required temperature. Time was allowed for the sample

to come to constant temperature before measurement was made; spectra were measured when temperature was constant within 0.3 °C for at least 15 minutes. Spectra were measured both for increasing and for decreasing series of temperatures.

To avoid saturation of the sample, the amplitude of the RF sweep field was kept at the lowest value for which a suitable signal could be obtained. The input power level was adjusted until the onset of saturation was noted and then reduced well below this level.

3.3. Differential Scanning Calorimetry

DSC measurements were performed on the Perkin Elmer Model DSC-1 differential scanning calorimeter using the low temperature accessory. The samples were encapsulated in pans usually used for solid samples, but, instead of the standard flat pan lid another pan with a slightly conically stretched wall was used as a lid. The encapsulation was not completely hermetical. Therefore the leak rate was determined and an eventual correction was considered in estimation of volatile adsorbate content. Sample holder domes were used in all measurements.

3.3.1. Preparation of samples

A sample of adsorbent (~0.5g) was placed in a small glass bulb provided with a stopcock, attached to the adsorption apparatus and degassed in the same way as the samples for NMR measurements. Benzene vapor was then condensed on the adsorbent at a temperature of about 10 °C until it was completely immersed in liquid benzene. The appropriate amount (~10mg) of adsorbent was then taken from the liquid and placed into the sample pan which was immediately covered with a stretched pan.

Just before the DSC measurement the weight of the pan with the sample was determined at several time intervals at room temperature to estimate the leak rate.

3.3.2. Measurements

Measurements were done at two scan speeds, 10 °C/min. and 2.5 °C/min., for all samples.

The pan was weighed immediately after the measurement and correction was eventually made to estimate the amount of adsorbate at the time of measurement. The lid of the pan was then perforated and adsorbed benzene removed by heating at 200 °C in vacuum for 2 hours. Weighing the pan with adsorbent and again after adsorbent was removed, the weight of adsorbent was determined.

4. Results and Interpretation

4.1. NMR Measurements

The proton NMR spectra were measured for several systems benzene / adsorbent listed in Table II., together with values of benzene adsorption given in g of benzene per g of degassed adsorbent and monolayer coverage relative to nitrogen BET area values. The molecular area of benzene is taken as 43.0 \AA^2 (36).

Table II

<u>Adsorbent</u>	<u>Benzene adsorption (g/g)</u>	<u>No. of Monolayers</u>
Charcoal	0.669	3.2
	0.682	3.3
	1.016	4.9
Silica gel	0.292	1.4
	0.388	1.8
Cab-o-sil	0.058	1.1
	0.250	4.5

The values of adsorption given are not corrected for the amount of adsorbate in the free volume of the NMR sample tube. The corrections were estimated by means of the equation

$$n_a = n - (V_g/RT) \cdot P(T, a)$$

where n is the total number of moles of an adsorbate present in the sample tube, n_a is the number of moles adsorbed, V_g is the free volume of the sample tube, and P is the vapor pressure in the sample tube, which depends on the temperature T and the specific adsorption a .

It was found that corrections are less than 2% for all systems, except for the systems benzene / Cab-o-sil, where the correction can

be about 22% and 30% for the fractional monolayer coverages 4.5 and 1.1, respectively.

For the charcoal systems both absorption and dispersion spectra were scanned at various temperatures, and heights of peaks and line widths at half-heights were evaluated.

For the silica systems the integrals were scanned additionally, using the built-in electronic integrator, and integrated intensities were evaluated, usually, as an average from three repetitive scans.

The lowest reachable temperature was limited by instrument design, and was about 160 °K.

The results for individual adsorption systems are summarized in a series of graphs representing the dependence of the NMR signal intensity on temperature, the effect of temperature on the NMR line width and the effect of temperature on the relative amount of the mobile phase.

The last quantity has been evaluated from the expression

$$C = I_T / 300 I_{300}$$

where I is the signal intensity (in arbitrary units) at temperature T , and I_{300} is the intensity, in the same units, at temperature 300 °K. The quantity C has a meaning of concentration of the mobile phase in the effective volume of the receiver coil, relative to concentration at 300 °K, if the temperature dependence is given only by the Curie law. Assuming that at 300 °K all adsorbate is present as the mobile phase, C is, with good approximation, measure of the relative amount of the mobile phase.

Where two symbols are used to indicate points in graphs, then + refers to descending temperatures, and x refers to ascending temperatures.

4.1.1. System benzene / charcoal

The results for three samples with fractional monolayer coverages 3.2, 3.3 and 4.9 are presented in Figs. 1-9. Because of broader line widths, as can be seen from Figs. 2, 5, and 8, the errors in intensities are greater for this system than for the others. For the range of line widths 1400 to 2400 Hz and the usable frequency sweep of spectrometer 8000 Hz, the errors evaluated from the equation (36) are about 4% and 20%, respectively, or about 20% if the concentrations corresponding to the line widths 1400 and 2400 Hz are compared.

Figs. 1-9 show that the temperature dependence of all plotted quantities shows hysteresis in the cooling-reheating cycle for all three samples. The content of the more mobile phase at the same temperature is higher for descending temperatures, as can be seen from Figs. 3, 6 and 9.

The same Figures show that the content of the more mobile phase starts to decrease at certain temperature, and the decreasing proceeds with decreasing temperature.

4.1.2. System benzene / silica gel

Figs. 10-15 show the results for two samples with benzene content of 0.292 and 0.388 g/g of adsorbent.

Figs. 13 and 15 for sample 0.388 g/g show a sharp decrease of the intensity and the mobile phase concentration at a temperature about 278 °K. A similar sharp decrease, but smaller, can be seen on

BENZENE / CHARCOAL 0.669 G/G

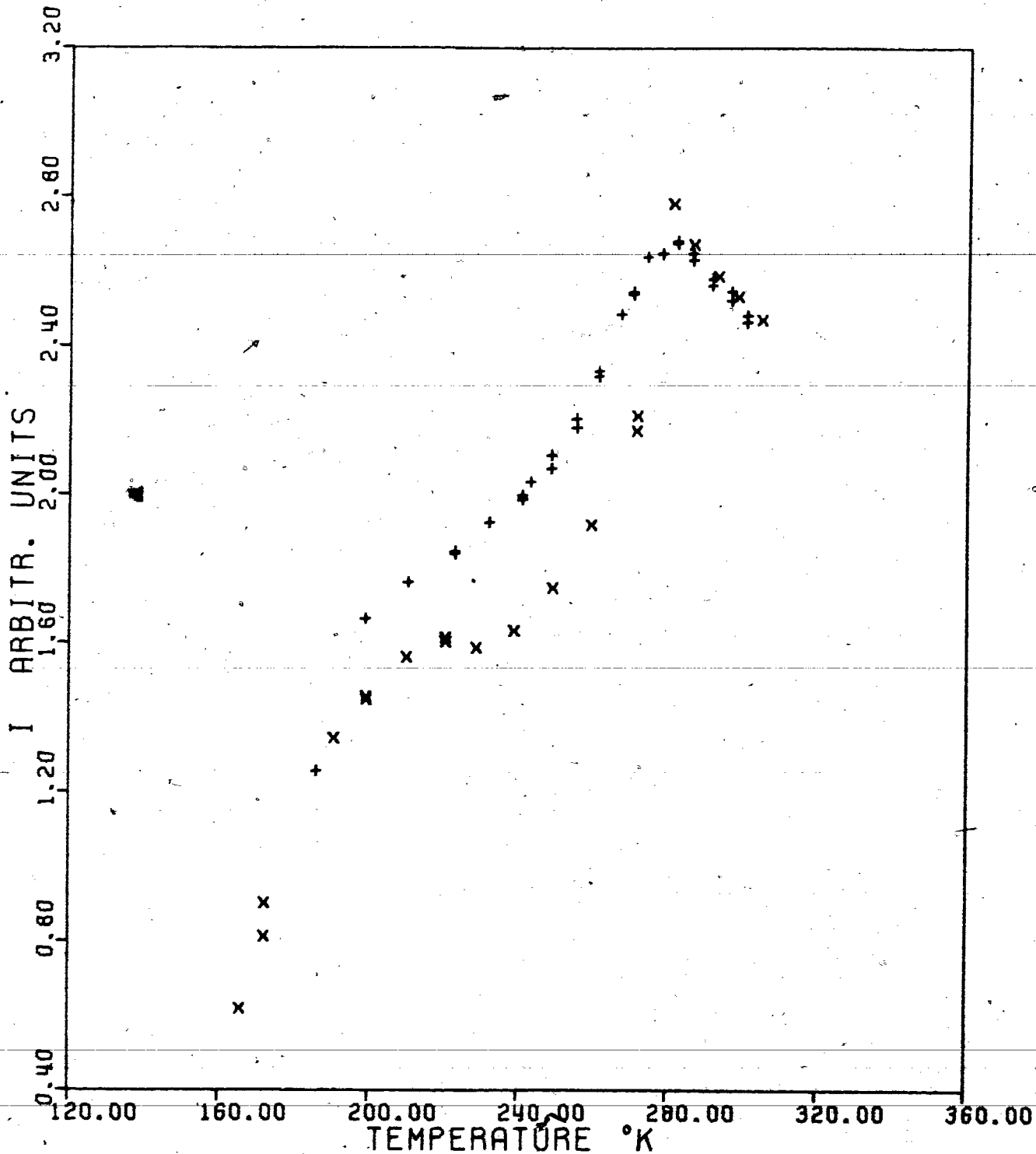


Fig. 1. The intensity of the NMR signal in arbitrary units as a function of temperature. System benzene / charcoal, 3.2 monolayers.

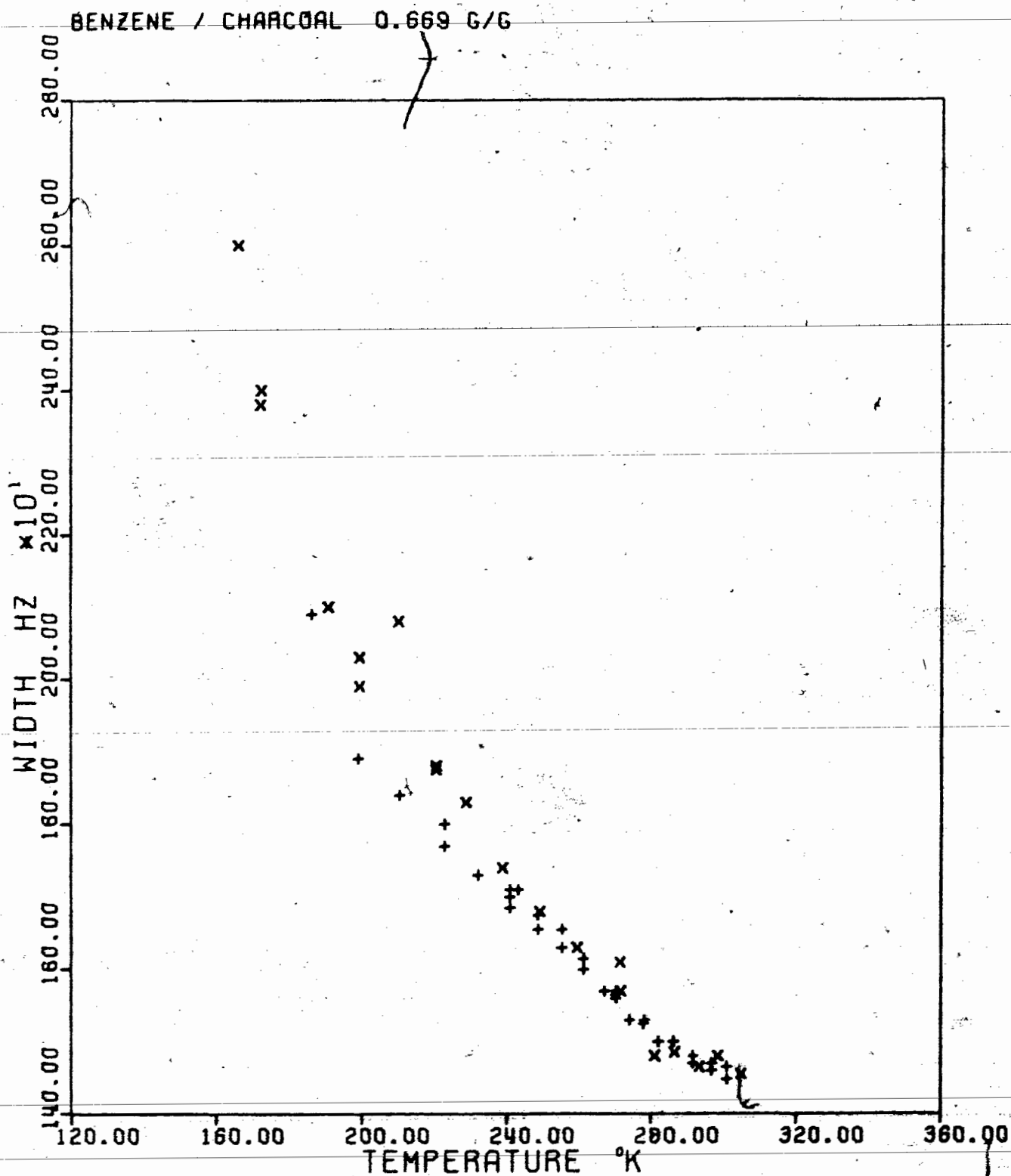


Fig. 2. Effect of temperature on the NMR line width at the half-maximum intensity. System benzene / charcoal: 3.2 monolayers.

BENZENE / CHARCOAL 0.669 G/G

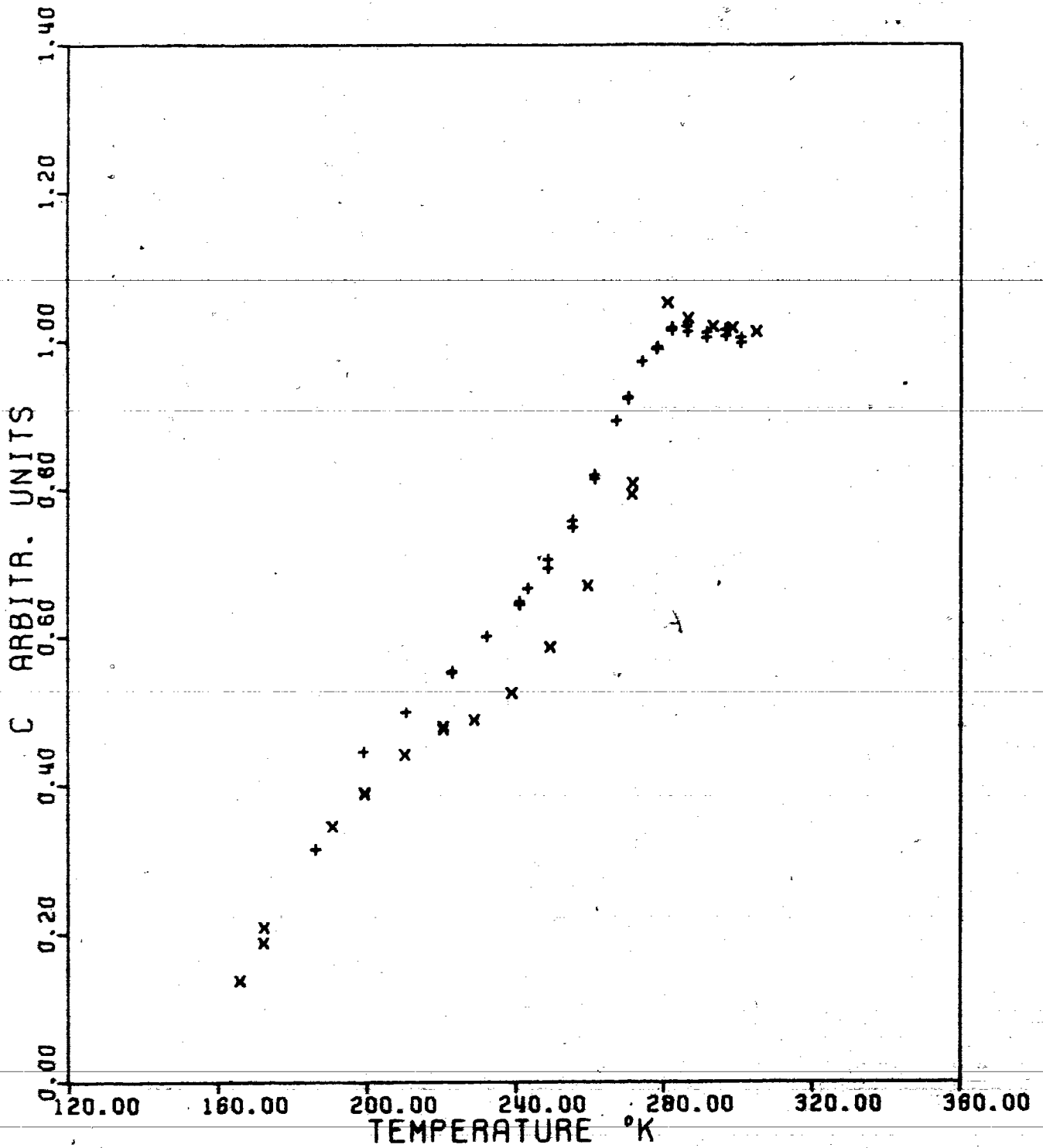


Fig. 3. Effect of temperature on the concentration of the mobile phase in arbitrary units. System benzene / charcoal, 3.2 monolayers.

BENZENE / CHARCOAL 0.682 G/G

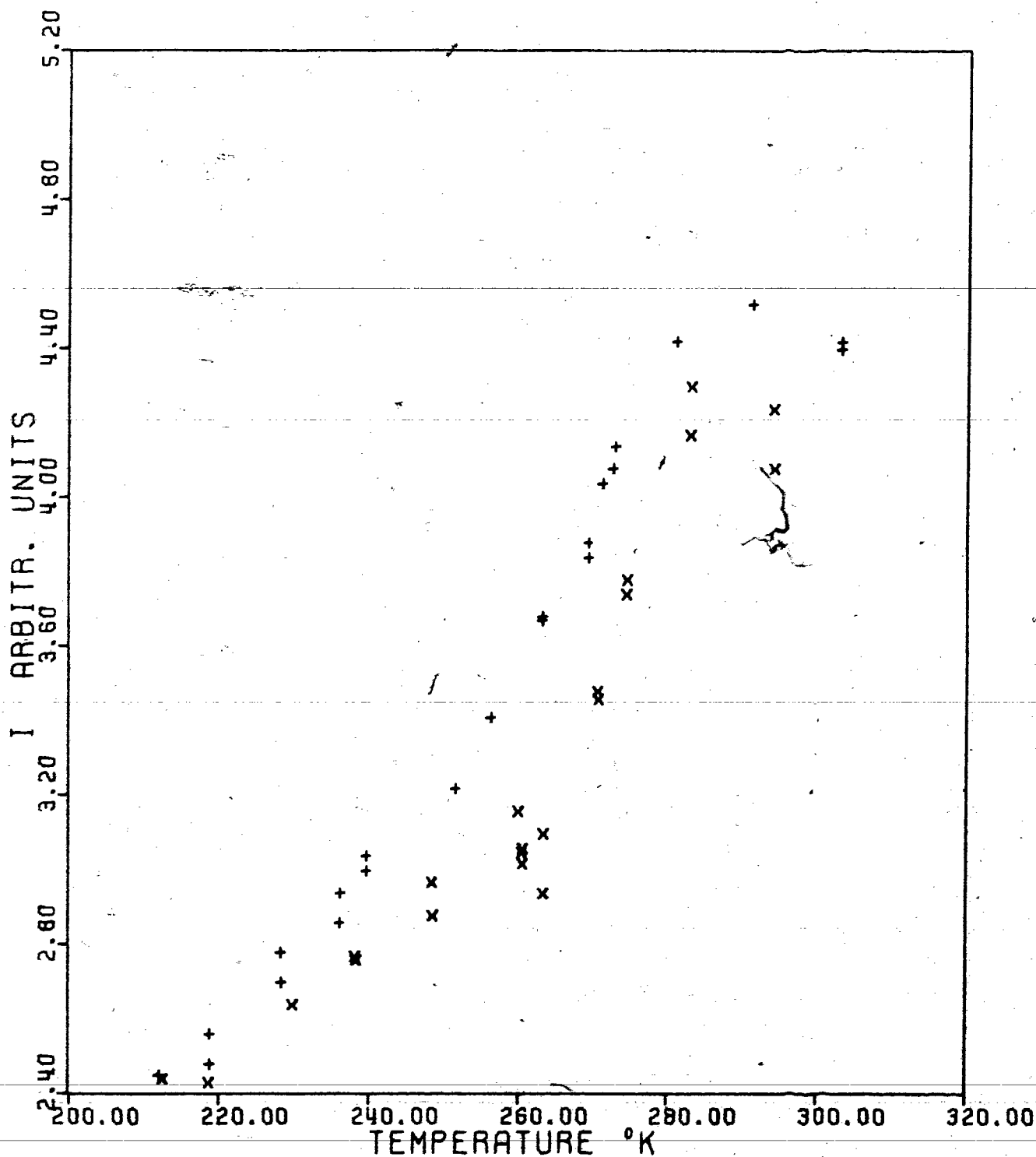


Fig. 4. The intensity of the NMR signal in arbitrary units as a function of temperature. System benzene / charcoal, 3.3 monolayers.

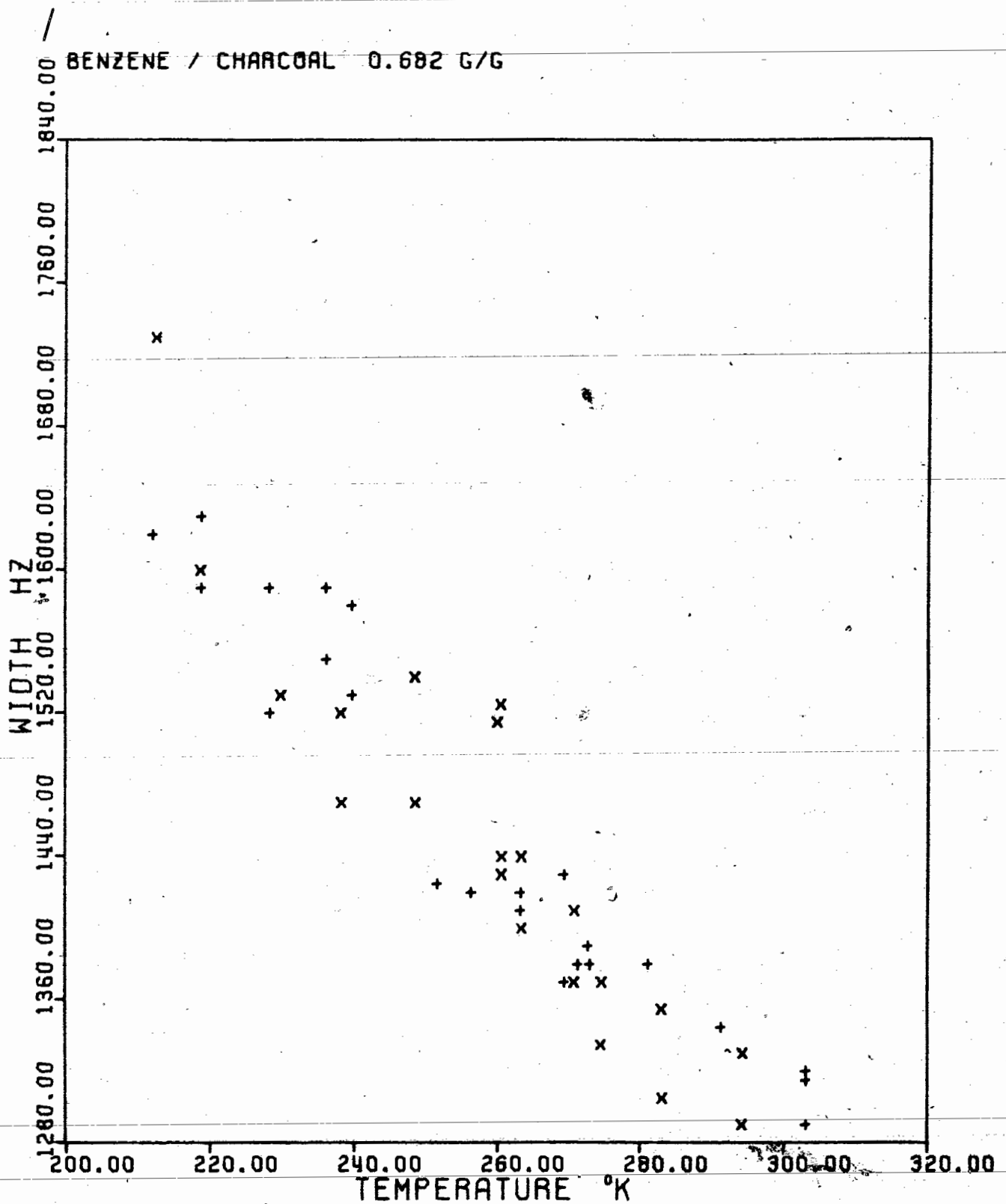


Fig. 5. Effect of temperature on the NMR line width at the half-maximum intensity. System benzene / charcoal 3.3 monolayers.

BENZENE / CHARCOAL 0.682 G/G

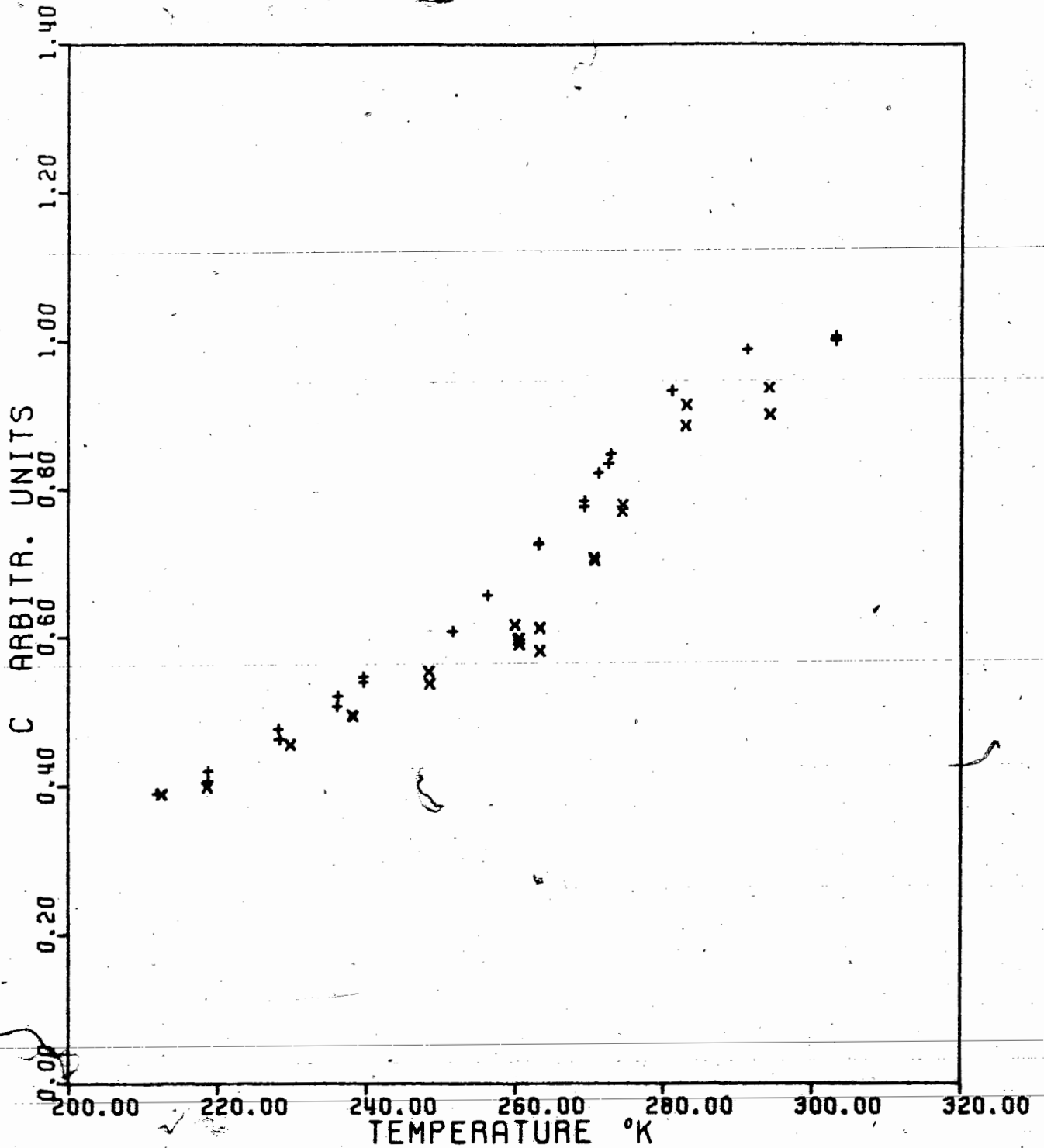


Fig. 6. Effect of temperature on the concentration of the mobile phase in arbitrary units. System benzene / charcoal, 3.3 monolayers.

BENZENE / CHARCOAL 1.016 G/G

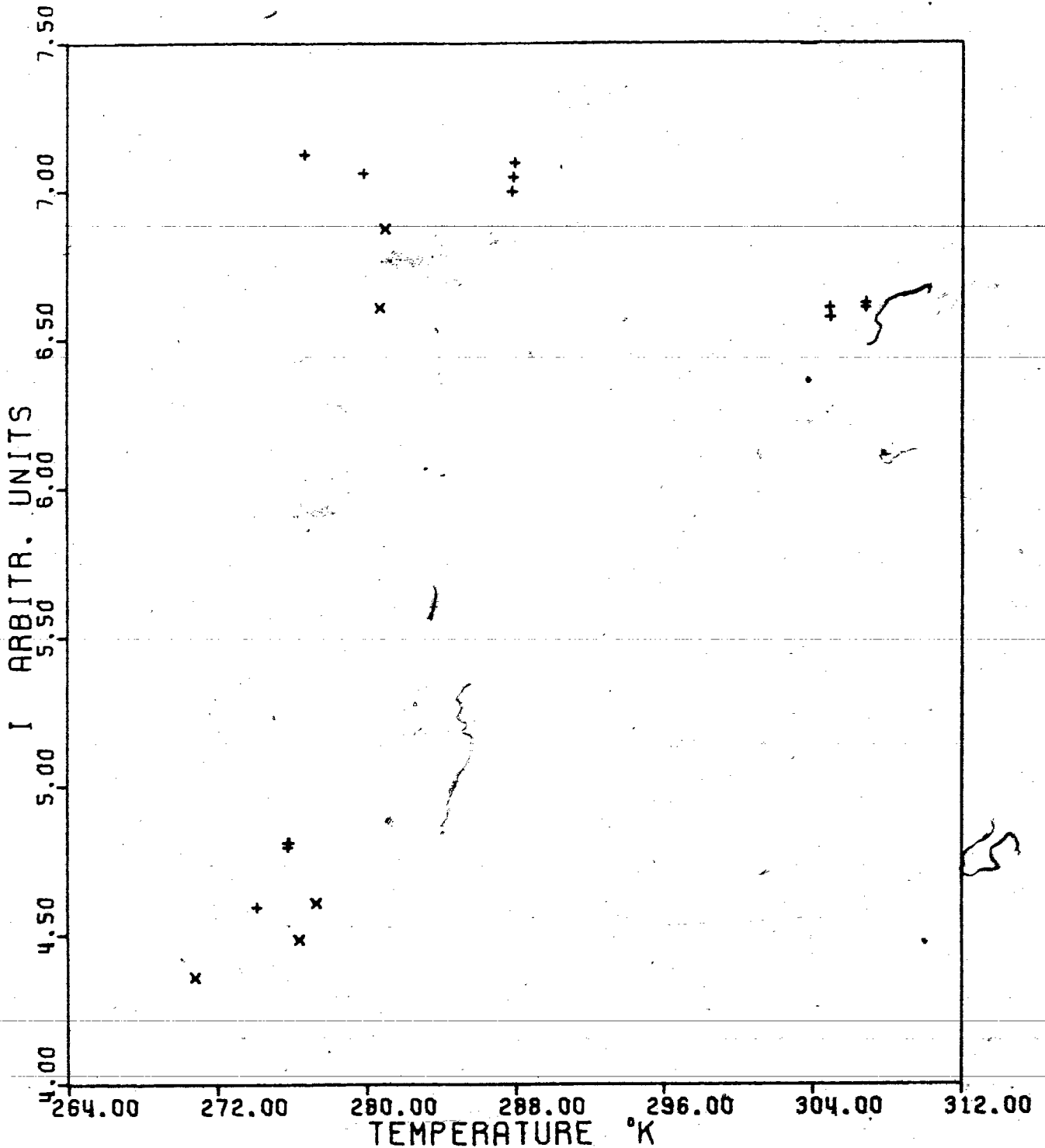


Fig. 7. The intensity of the NMR signal in arbitrary units as a function of temperature. System benzene / charcoal, 4.9 monolayers.

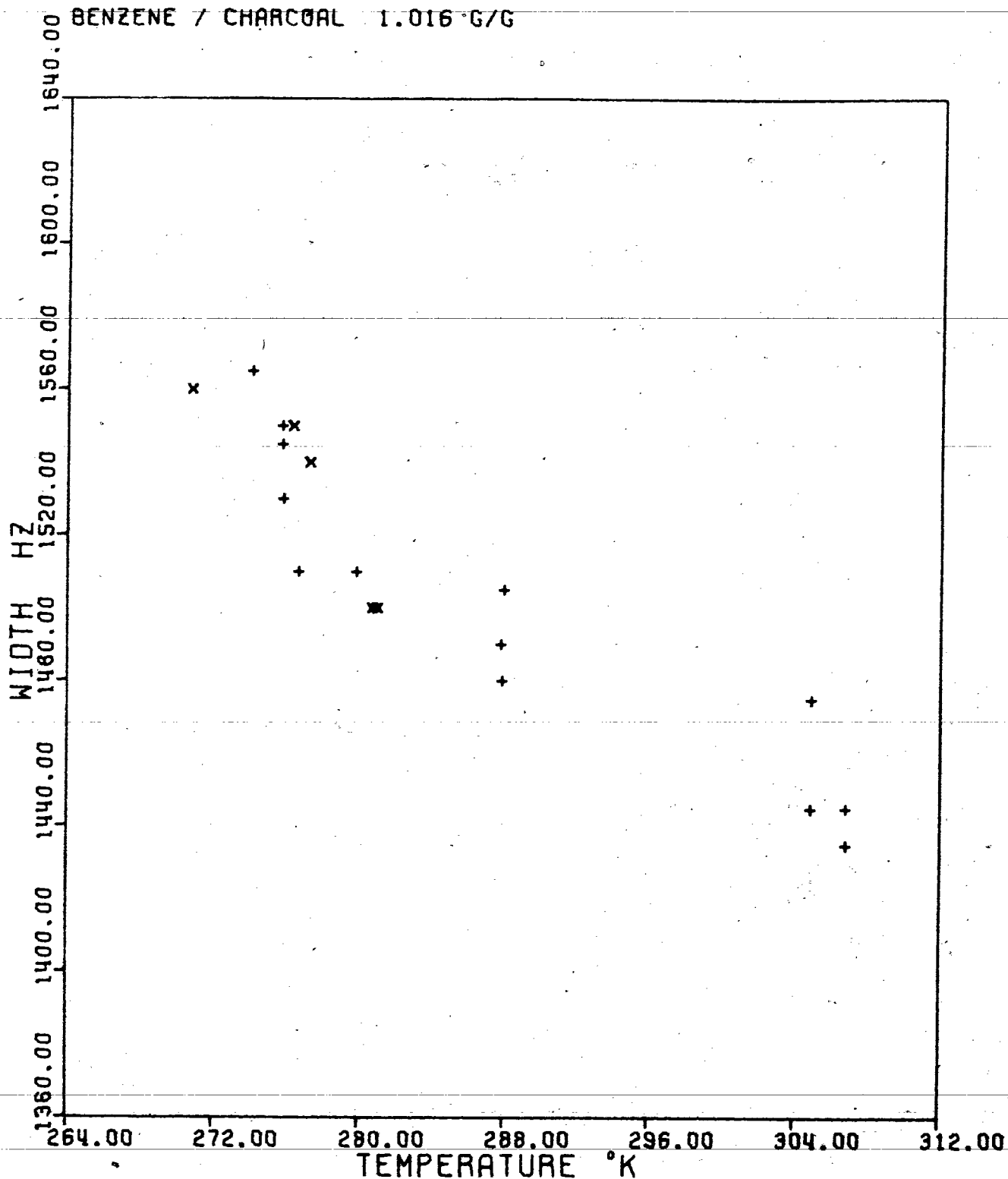


Fig. 8. Effect of temperature on the NMR line width at the half-maximum intensity. System benzene / charcoal 4.9 monolayers.

BENZENE / CHARCOAL 1.016 G/G

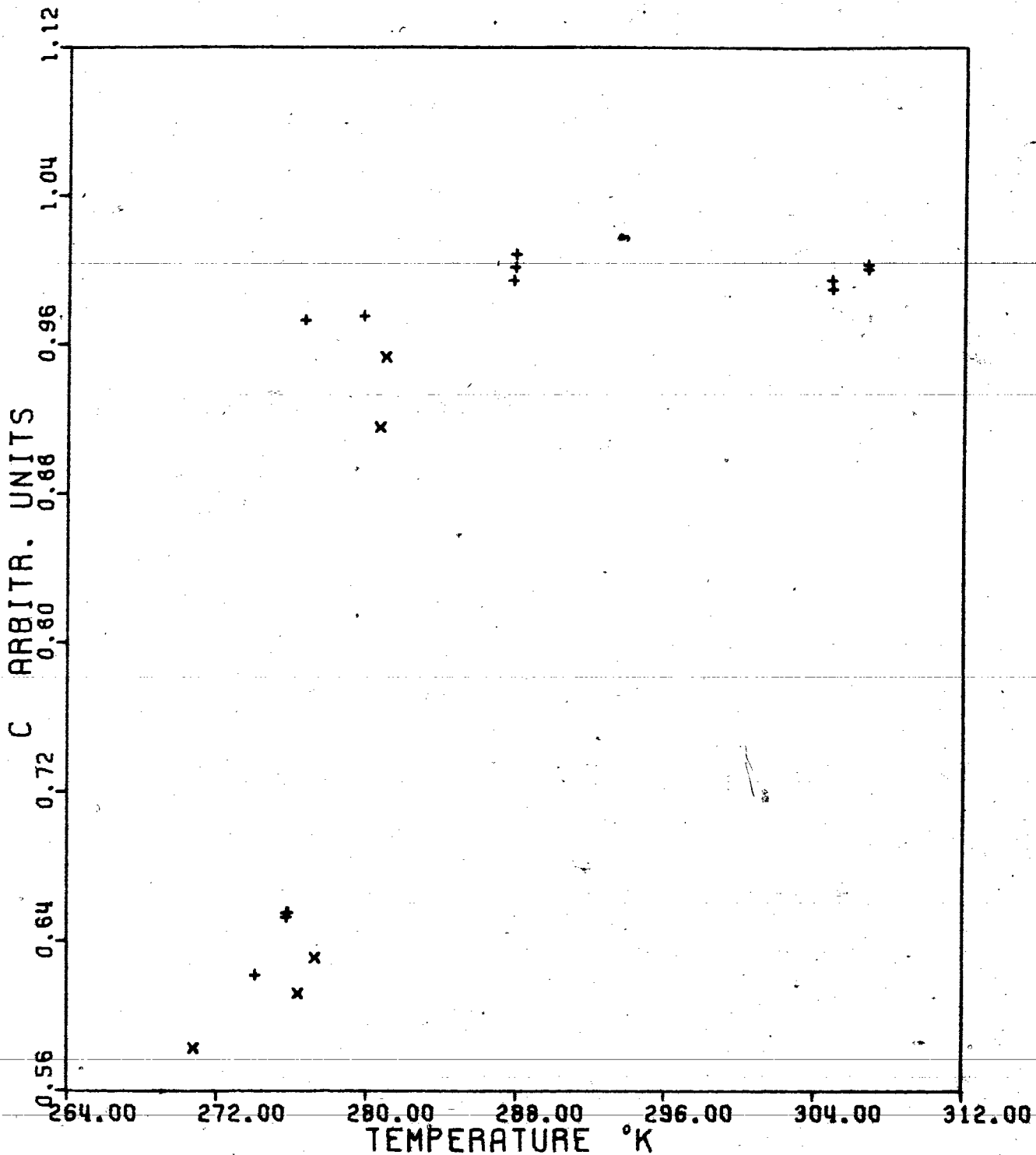


Fig. 9. Effect of temperature on the concentration of the mobile phase in arbitrary units. System benzene / charcoal, 4.9 monolayers.

BENZENE / SILICAGEL 0.292 G/G

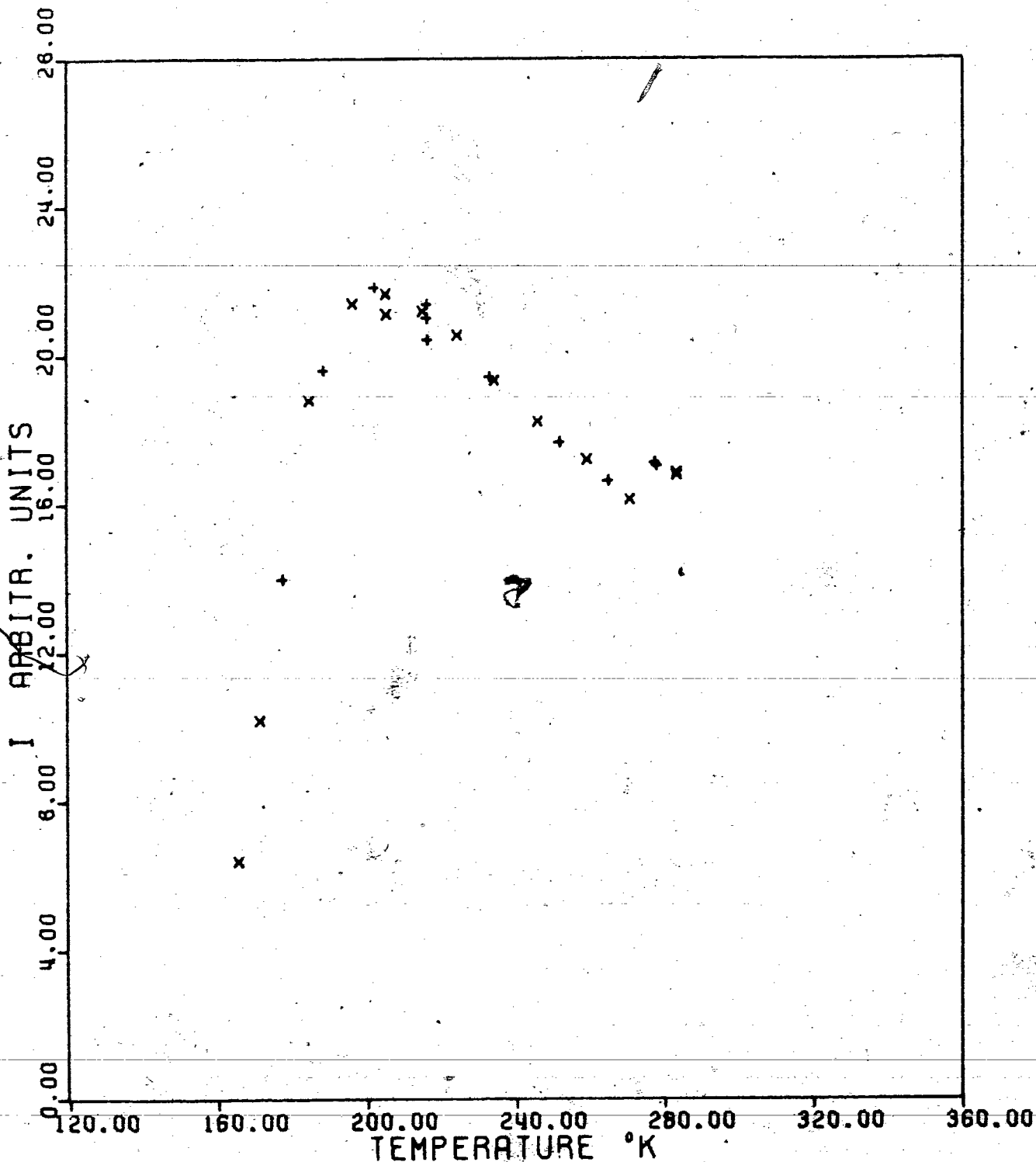


Fig. 10. The intensity of the NMR signal in arbitrary units as a function of temperature. System benzene / silicagel, 1.4 monolayers.

BENZENE / SILICAGEL 0.292 G/G

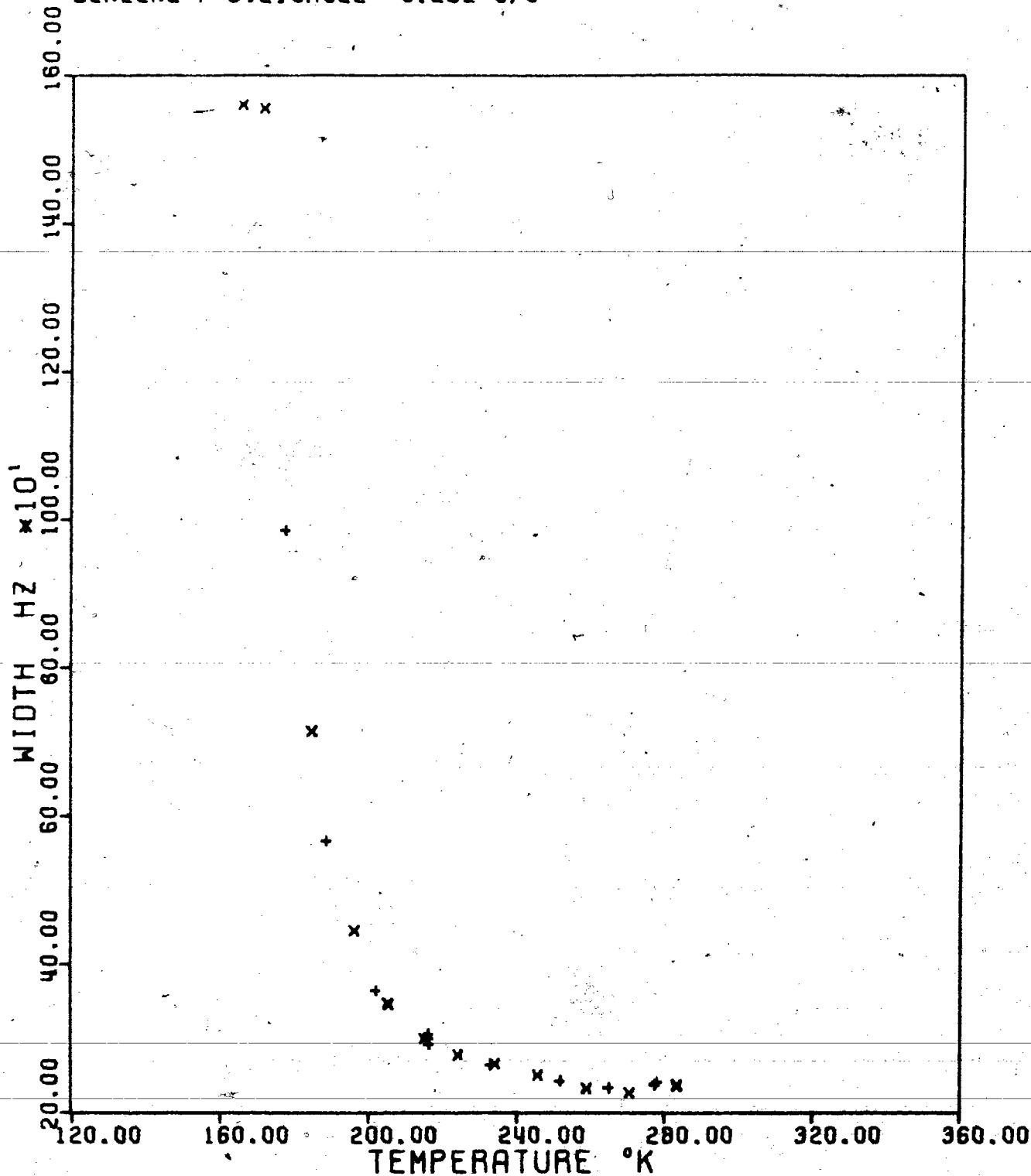


Fig. 11. Effect of temperature on the NMR line width at the half-maximum intensity. System benzene / silica gel 1.4 monolayers.

BENZENE / SILICAGEL 0.292 G/G

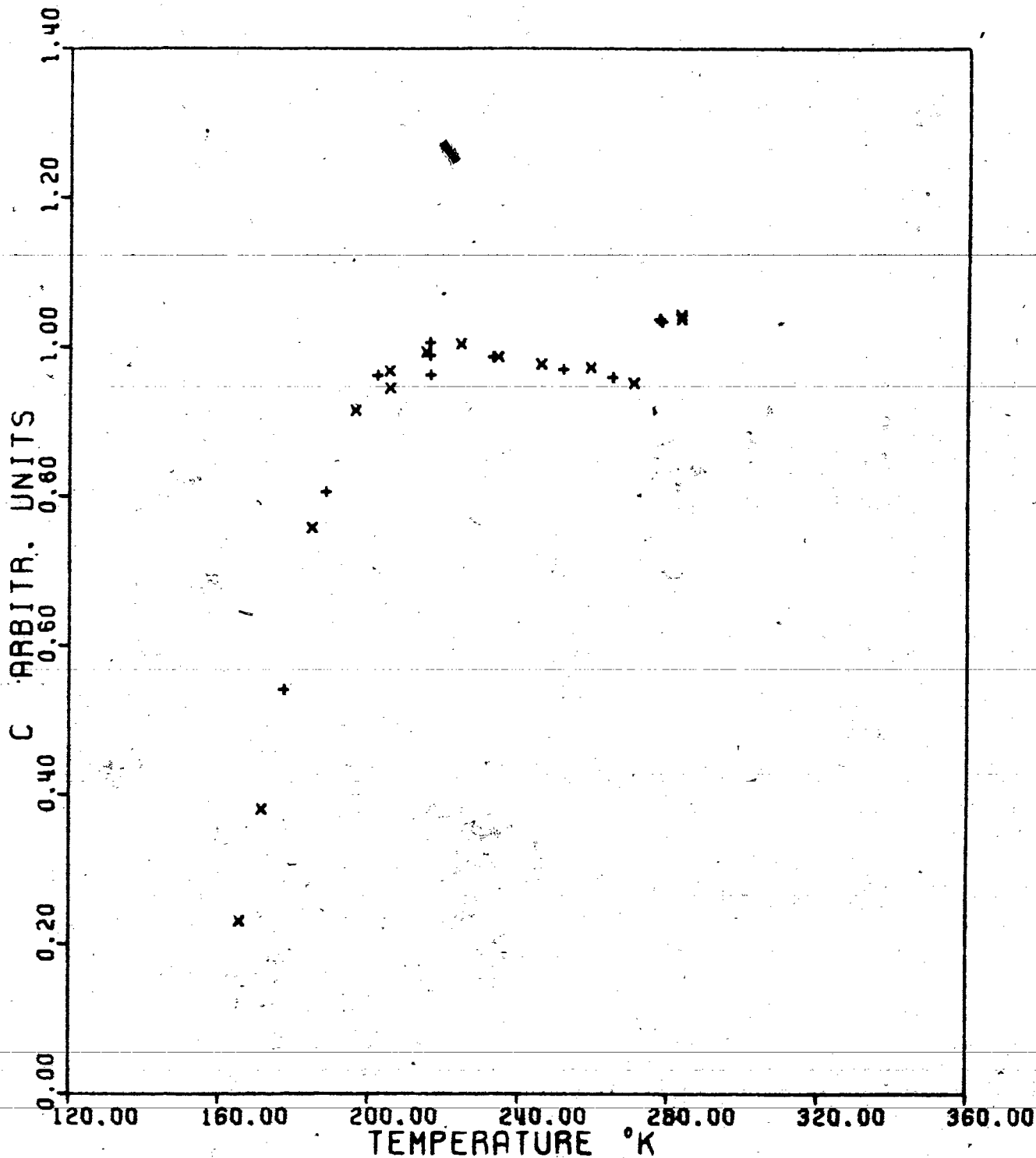


Fig. 12. Effect of temperature on the concentration of the mobile phase in arbitrary units. System benzene / silica gel, 1.4 monolayers.

BENZENE / SILICAGEL 0.388 G/G

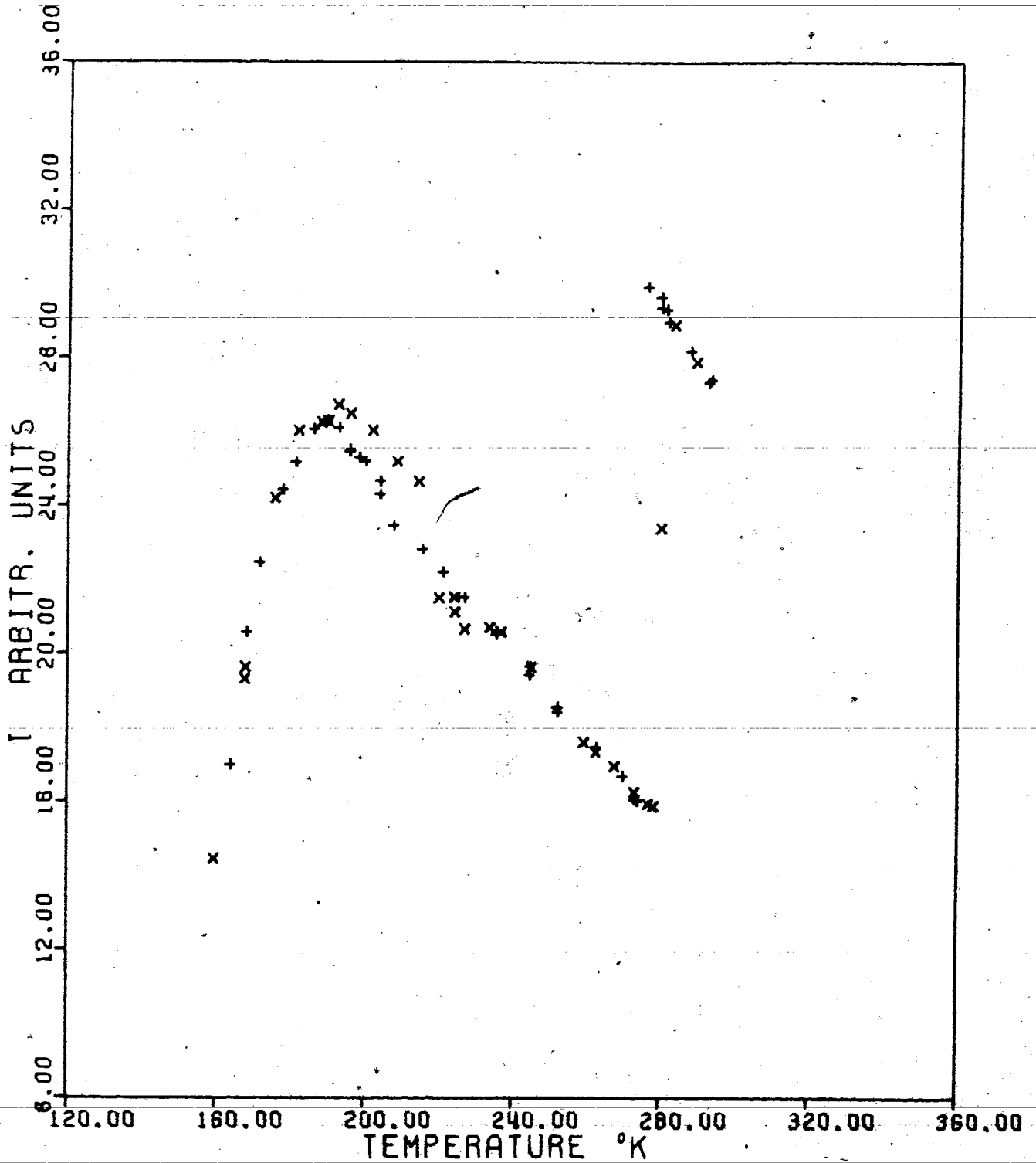


Fig. 13. The intensity of the NMR signal in arbitrary units as a function of temperature. System benzene / silicagel, 1.8 monolayers.

BENZENE / SILICAGEL 0.388 G/G

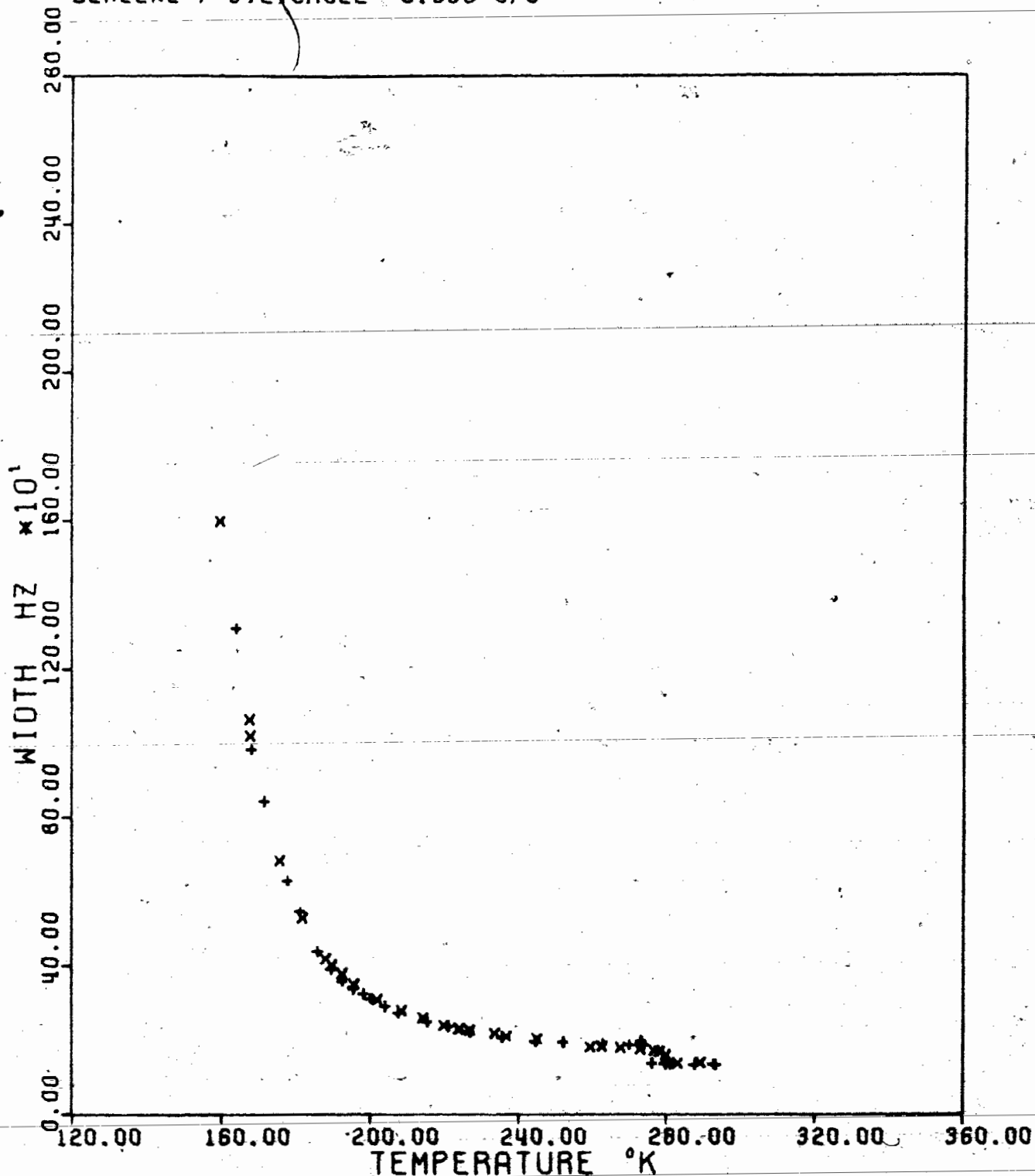


Fig. 14. Effect of temperature on the NMR line width at the half-maximum intensity. System benzene / silica gel 1.8 monolayers.

BENZENE / SILICAGEL 0.388 G/G

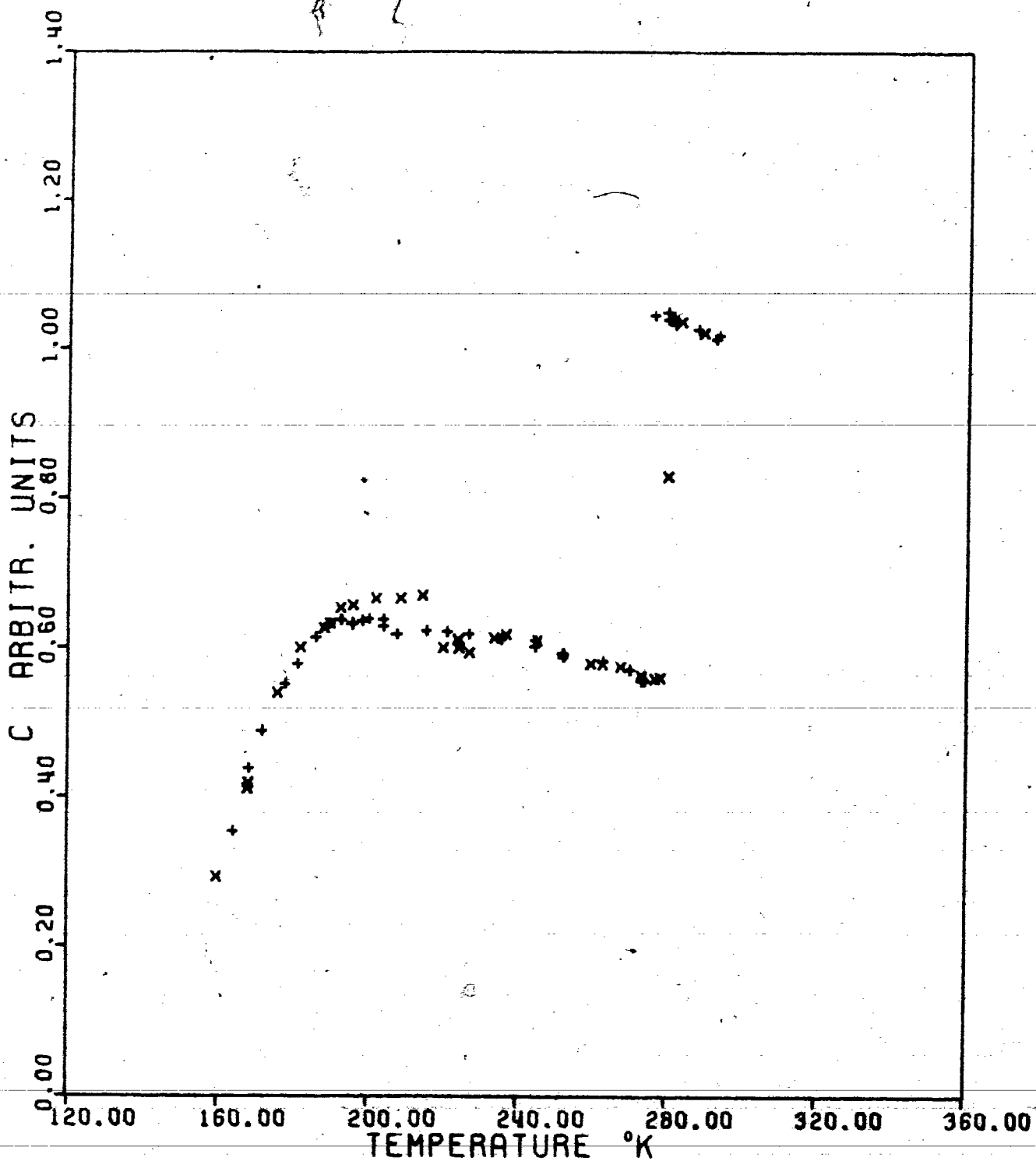


Fig. 15. Effect of temperature on the concentration of the mobile phase in arbitrary units. System benzene / silica gel, 1.8 monolayers.

Figs. 10 and 12 for the sample 0.292 g/g. The course of the temperature dependence of the line widths is practically unchanged, as Figs. 11 and 14 show.

As can be seen from Figs. 12 and 15, after the sharp decrease the amount of the mobile phase is relatively constant (actually it is slightly increasing) over a rather extensive range of temperatures, and then starts gradually to decrease.

The slight increase in the amount of the mobile phase can only partly be explained by additional adsorption from the gas phase in the free volume of the NMR sample tube. The other reasons may be the temperature dependence of instrumental factors or the redistribution of adsorbate due to the temperature gradient in the NMR tube.

4.1.3. System benzene / Cab-o-sil

The results for two samples with fractional monolayer coverages 1.1 and 4.5 are presented in Figs. 16-21.

Because of smaller specific surface and specific volume weight (0.11 g/ml., to compare with 0.87 for silica gel and 0.40 g/ml for charcoal) of Cab-o-sil, the amounts of benzene present in NMR sample tube were smaller, and the amounts adsorbed were more subjected to the change of adsorption with temperature as can be seen from Figs. 18 and 21. Similarly, as for the silica gel systems, it seems that not all the increase is due to the change of adsorption with temperature.

Qualitatively the temperature dependence of the intensities and

BENZENE / CAB-O-SIL 0.058 G/G

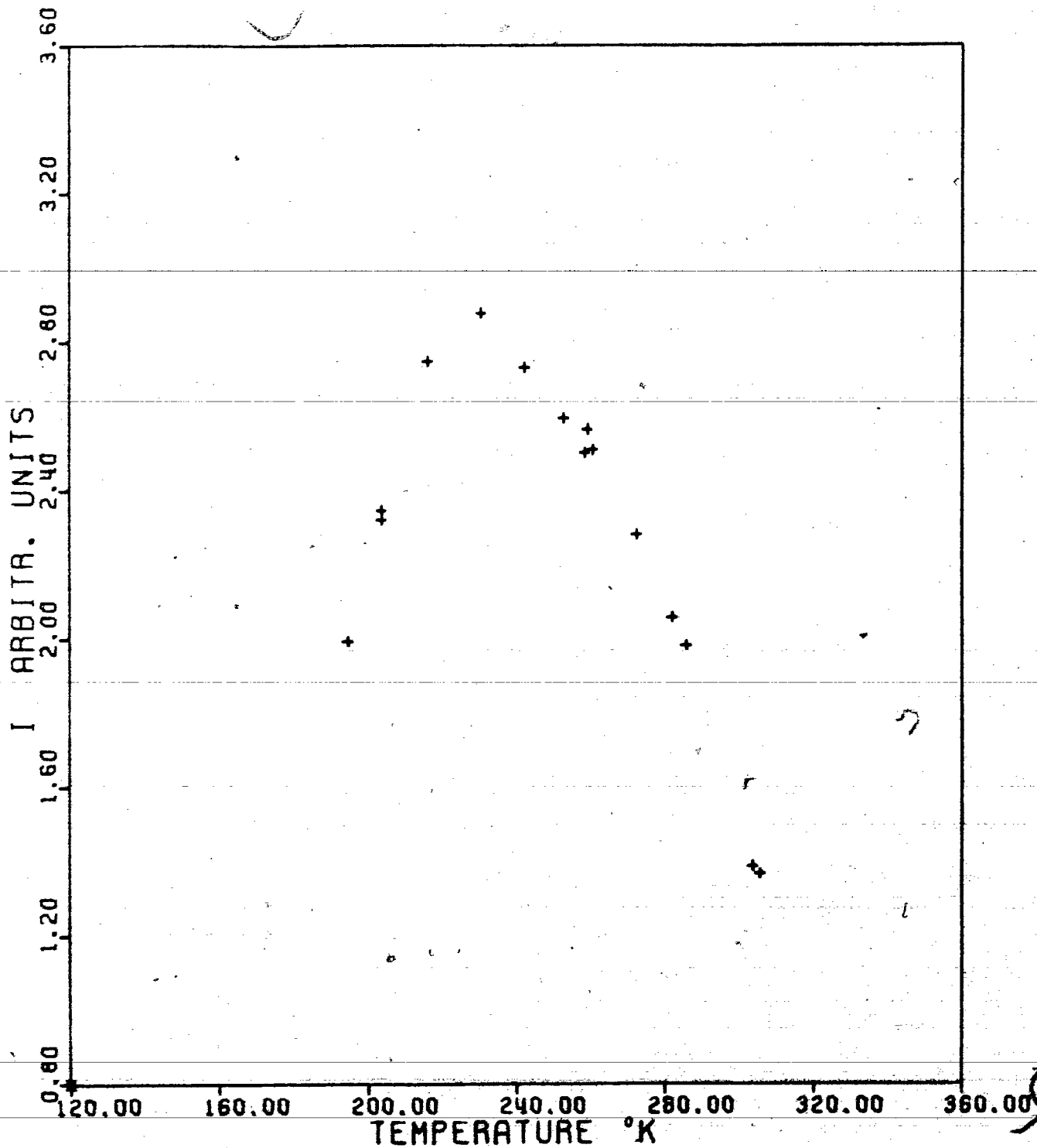


Fig. 16. The intensity of the NMR signal in arbitrary units as a function of temperature. System benzene / cab-o-sil, 1.1 monolayers.

BENZENE / CAB-O-SIL 0.058 G/G

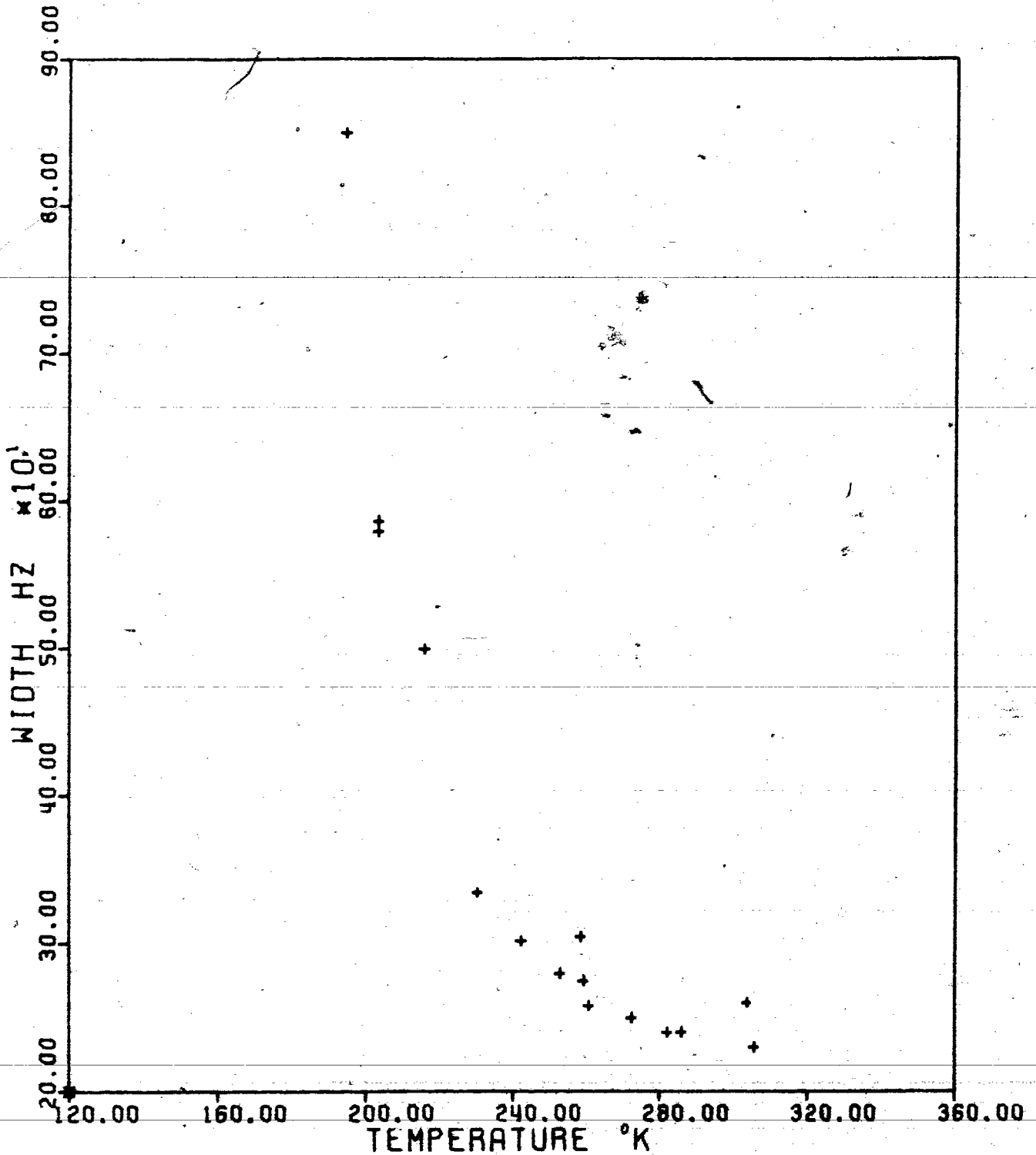


Fig. 17. Effect of temperature on the NMR line width at the half-maximum intensity. System benzene / cab-o-sil, 1.1 monolayers.

BENZENE / CAB-O-SIL 0.058 G/G

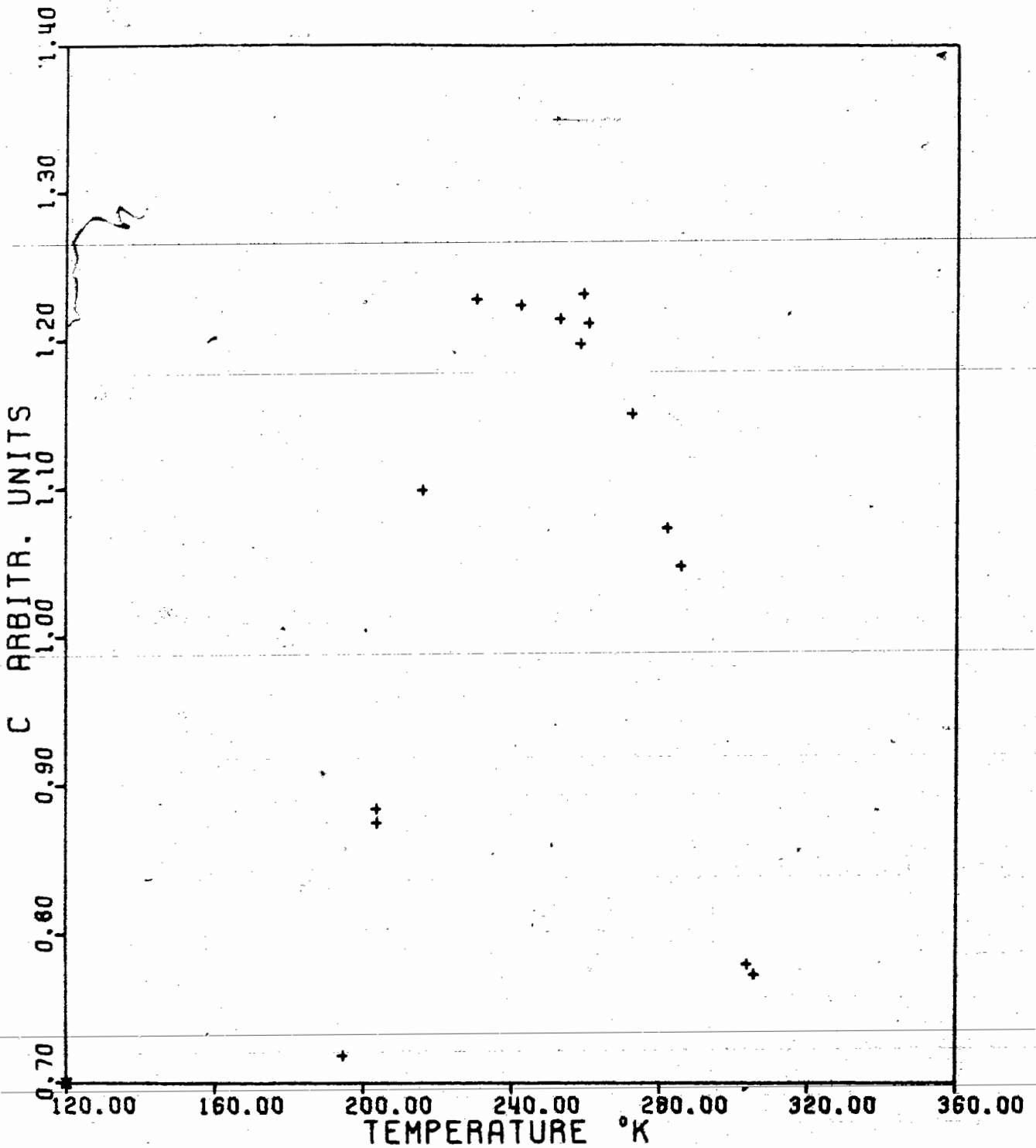


Fig. 18. Effect of temperature on the concentration of the mobile phase in arbitrary units. System benzene / cab-o-sil, 1.1 monolayers.

BENZENE / CAB-O-SIL 0.250 G/G

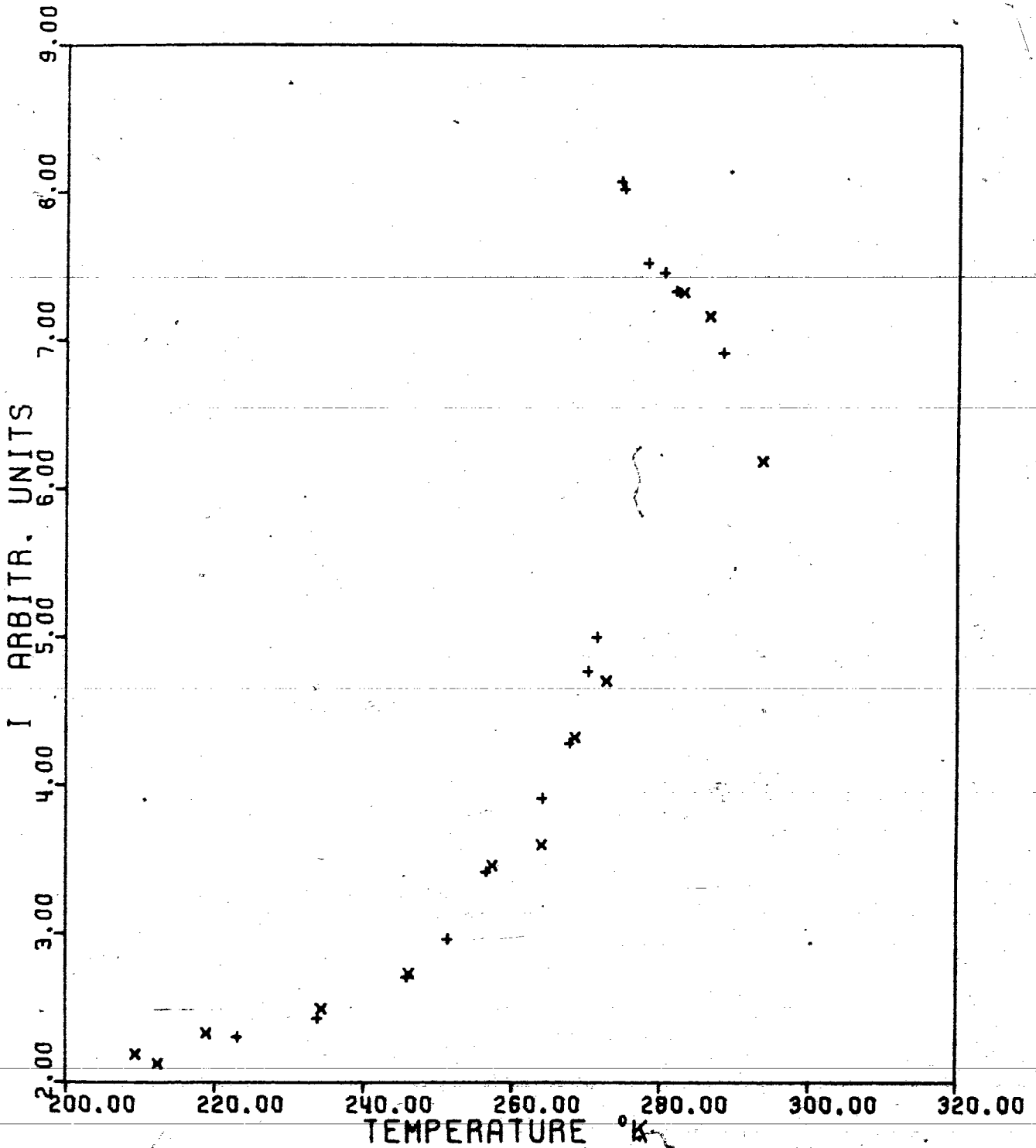


Fig. 19. The intensity of the NMR signal in arbitrary units as a function of temperature. System benzene / cab-o-sil, 4.5 monolayers.

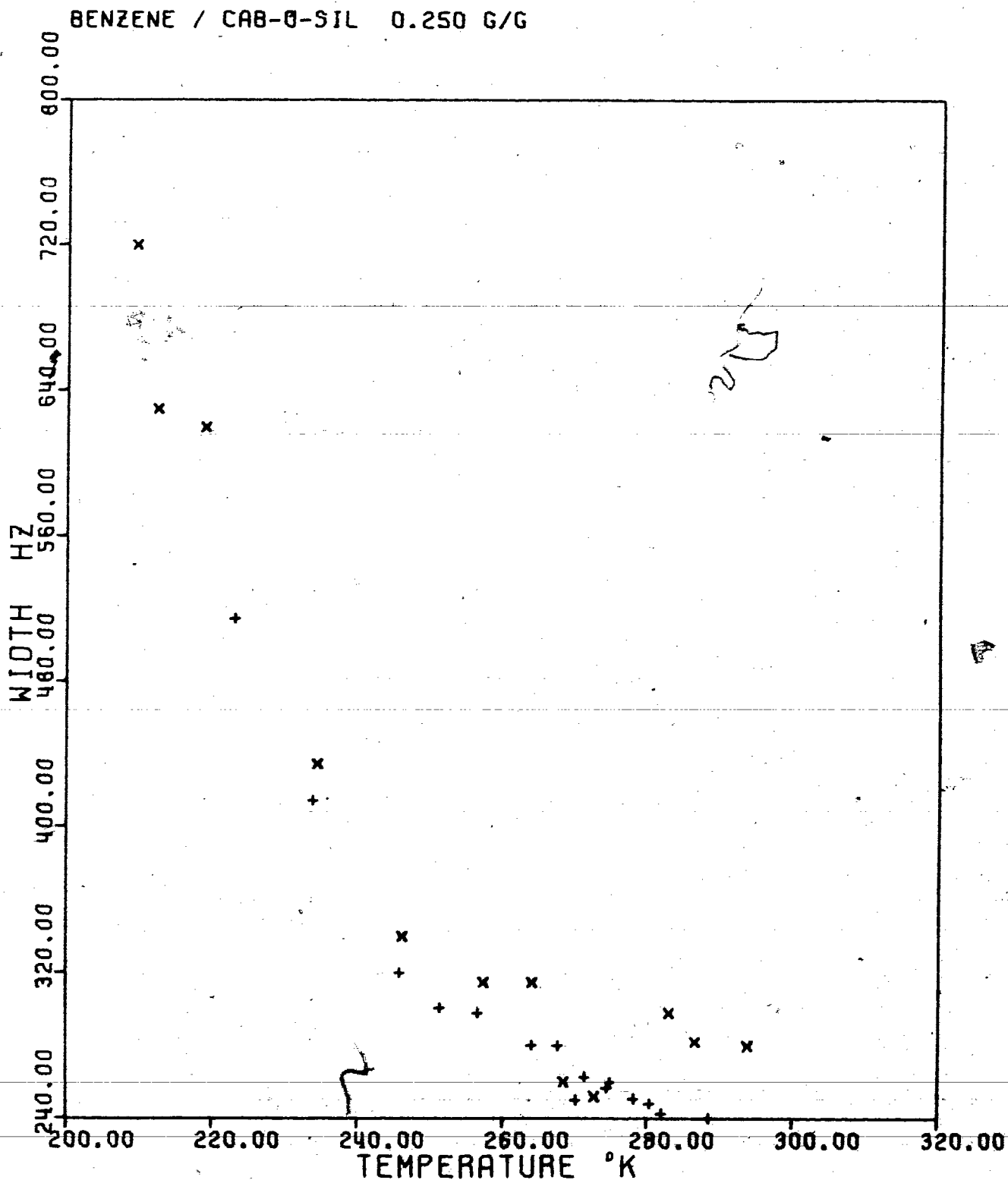


Fig. 20. Effect of temperature on the NMR line width at the half-maximum intensity. System benzene / cab-o-sil, 4.5 monolayers.

BENZENE / CAB-O-SIL 0.250 G/G

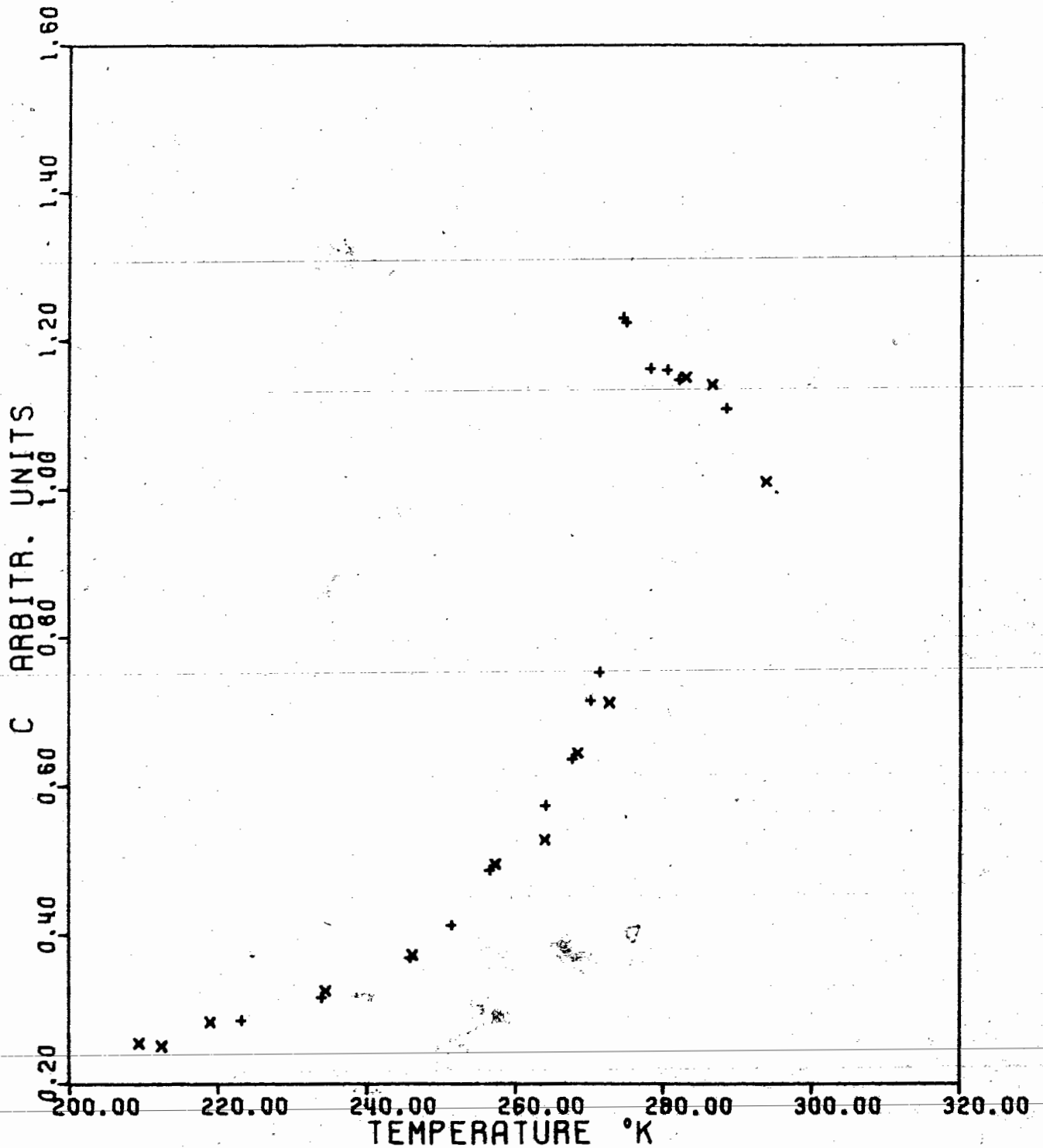


Fig. 21. Effect of temperature on the concentration of the mobile phase in arbitrary units. System benzene / cab-o-sil, 4.5 monolayers.

the amounts of mobile phase show similar features as for the system charcoal / benzene, the drop at the temperature about 278 K, and then gradual decrease with decreasing temperature.

4.2. DSC Measurements

Because of the problem with completely hermetical encapsulation of samples, the amounts of the adsorbate during the measurements were not known exactly. The values given are the arithmetic means calculated from the experimentally determined beginning and end amounts in the individual runs. The shown uncertainties were evaluated as half of the amount of adsorbate lost by evaporation during the measurement.

All the DSC curves shown represent the heating curves. The peaks on the cooling curves were unusually sharp and occurred at irreproducible temperatures, lower than those on the heating curves, thus indicating supercooling.

4.2.1. System benzene / charcoal

In Figs. 22-25 are shown DSC curves for system benzene / charcoal. The two scans of the sample 0.88 g of benzene / g of charcoal in Figs. 22-23 show that the behaviour of the system with increasing temperature is reproducible. Figs. 24 and 25 show DSC curves of the sample 0.79 g/g at scan speeds 10 °C/min. and 2.5 °C/min., respectively. As can be seen, the general features of the curves are the same; therefore it may be assumed that the curves reflect

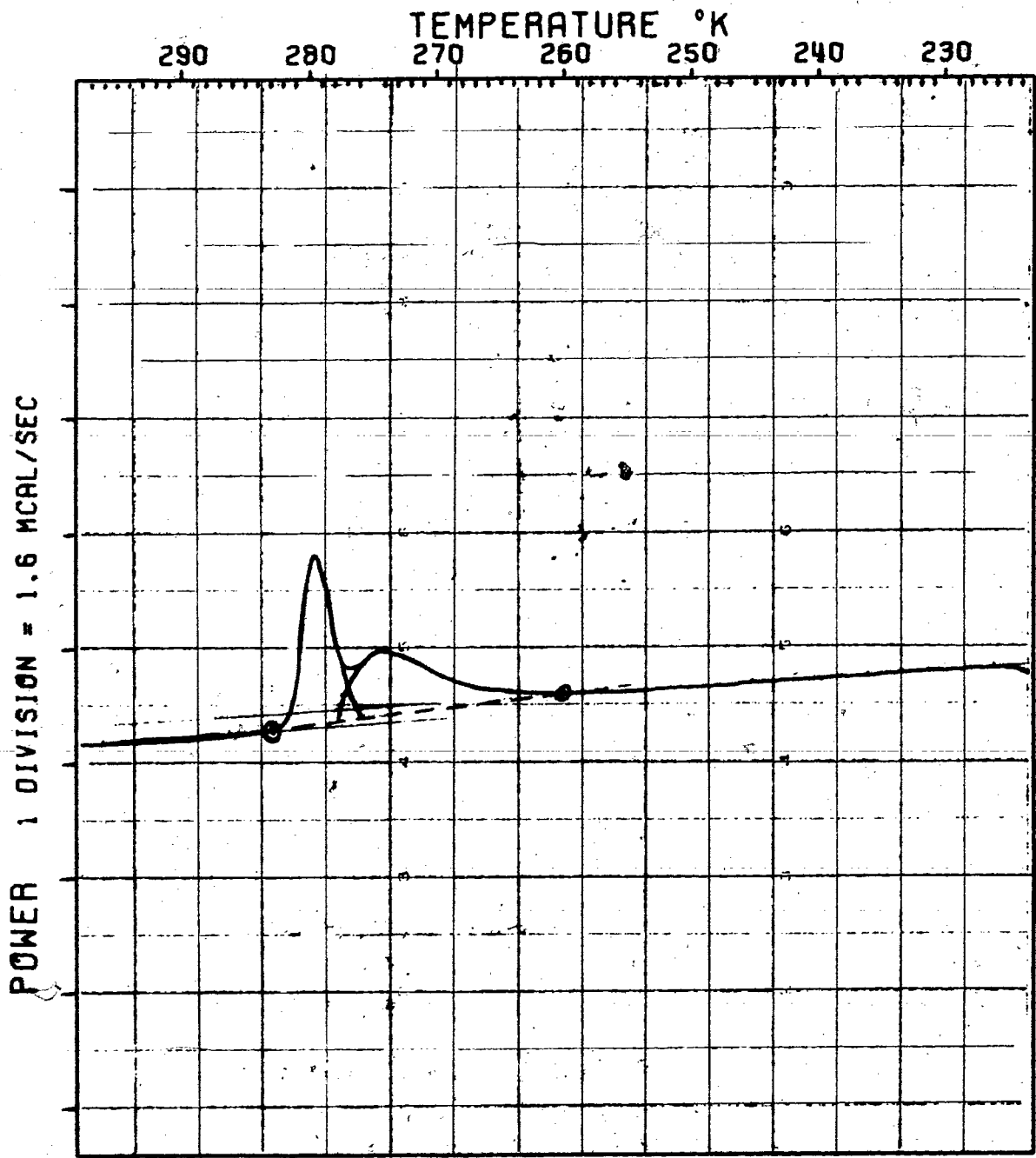


Fig. 22. DSC curve of the system benzene / charcoal 0.88 ± 0.04 g/g. Scan speed 10 °C/min. Range 1.6 mcal sec^{-1} inch^{-1} .

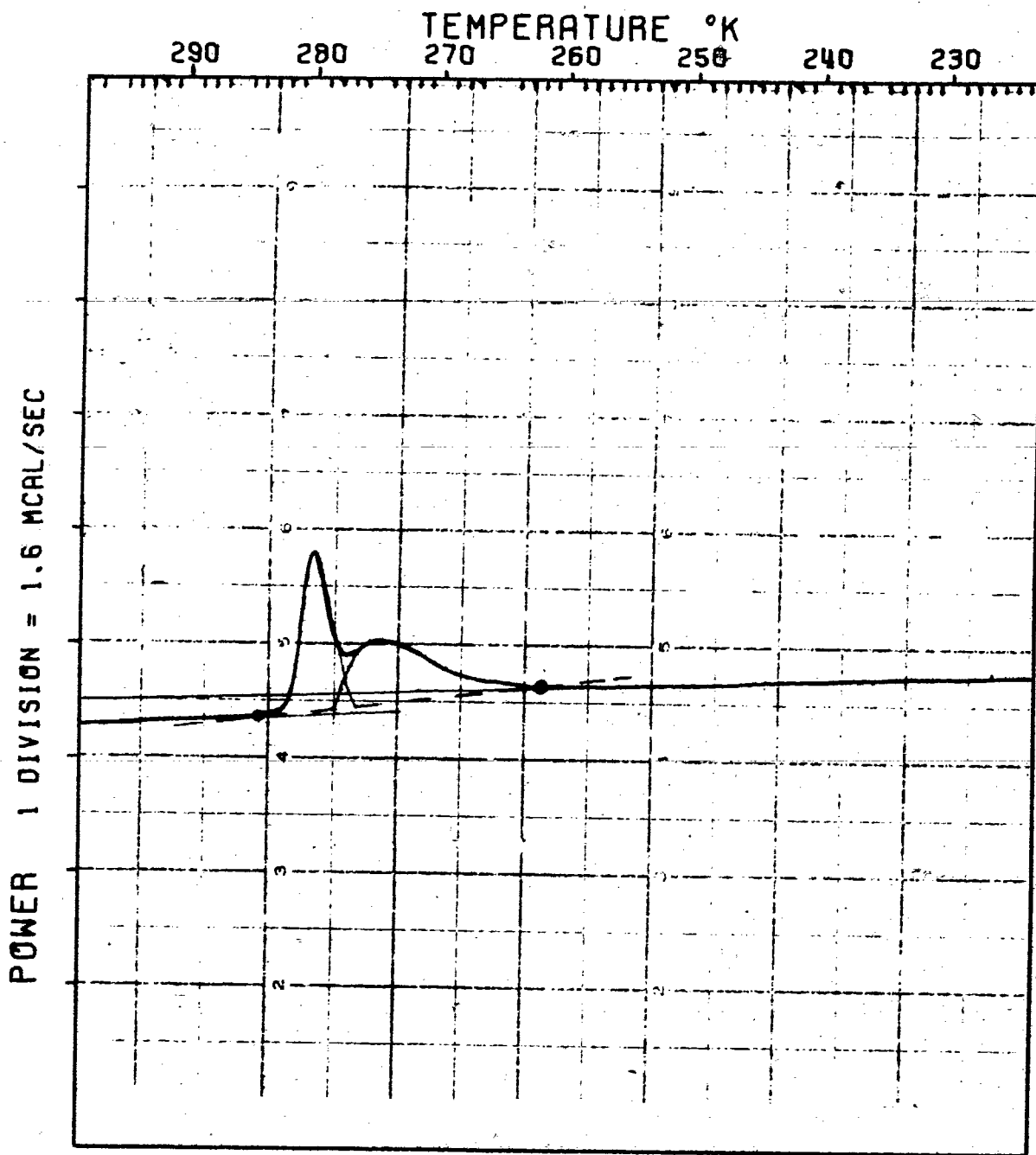


Fig. 23. DSC curve of the system benzene / charcoal 0.88 ± 0.04 g/g. Scan speed 10 °C/min. Range 1.6 mcal sec^{-1} inch^{-1} .

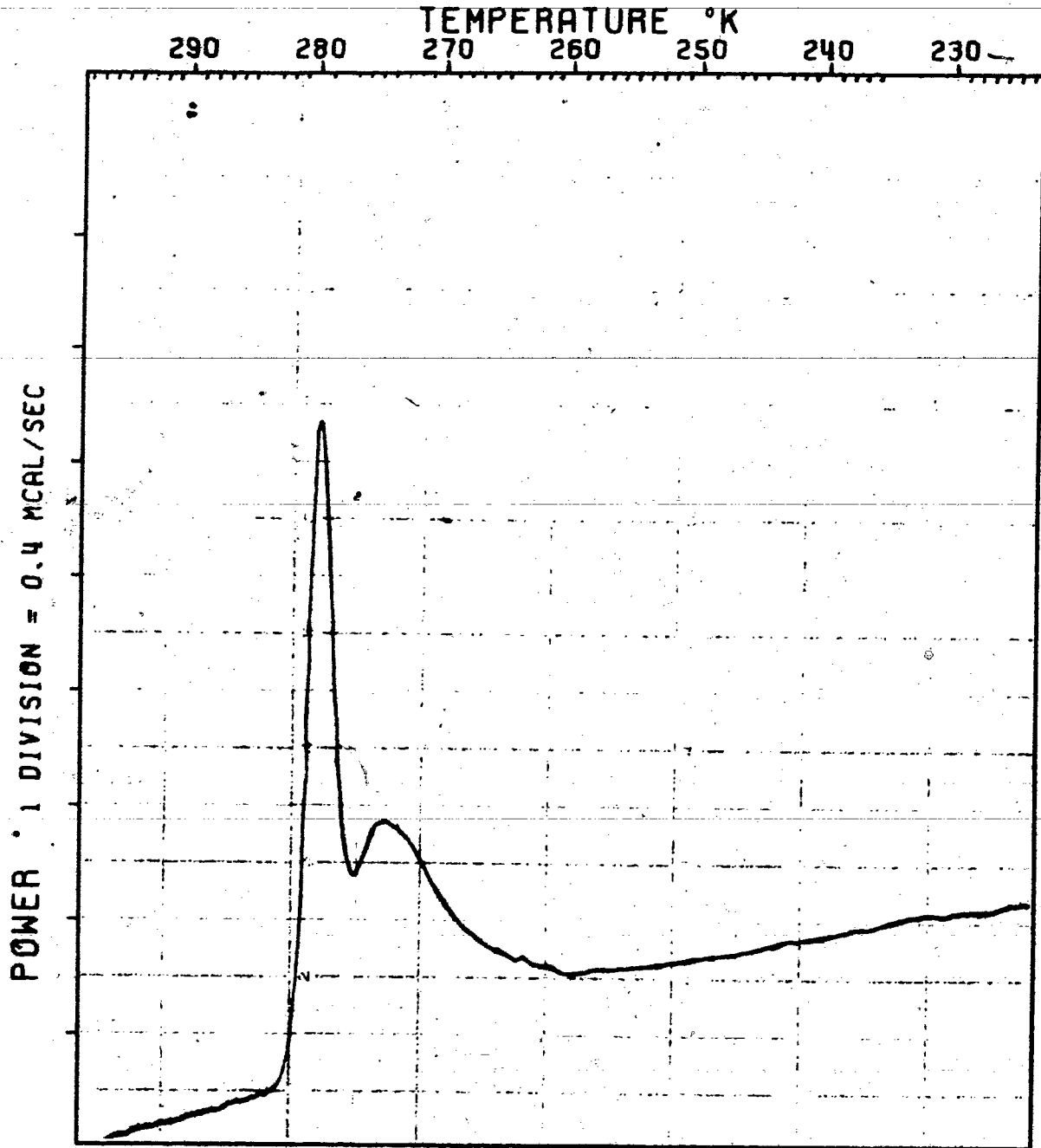


Fig. 24. DSC curve of the system benzene / charcoal 0.79 ± 0.03 g/g. Scan speed 10 °C/min. Range 0.4 mcal sec^{-1} inch^{-1} .

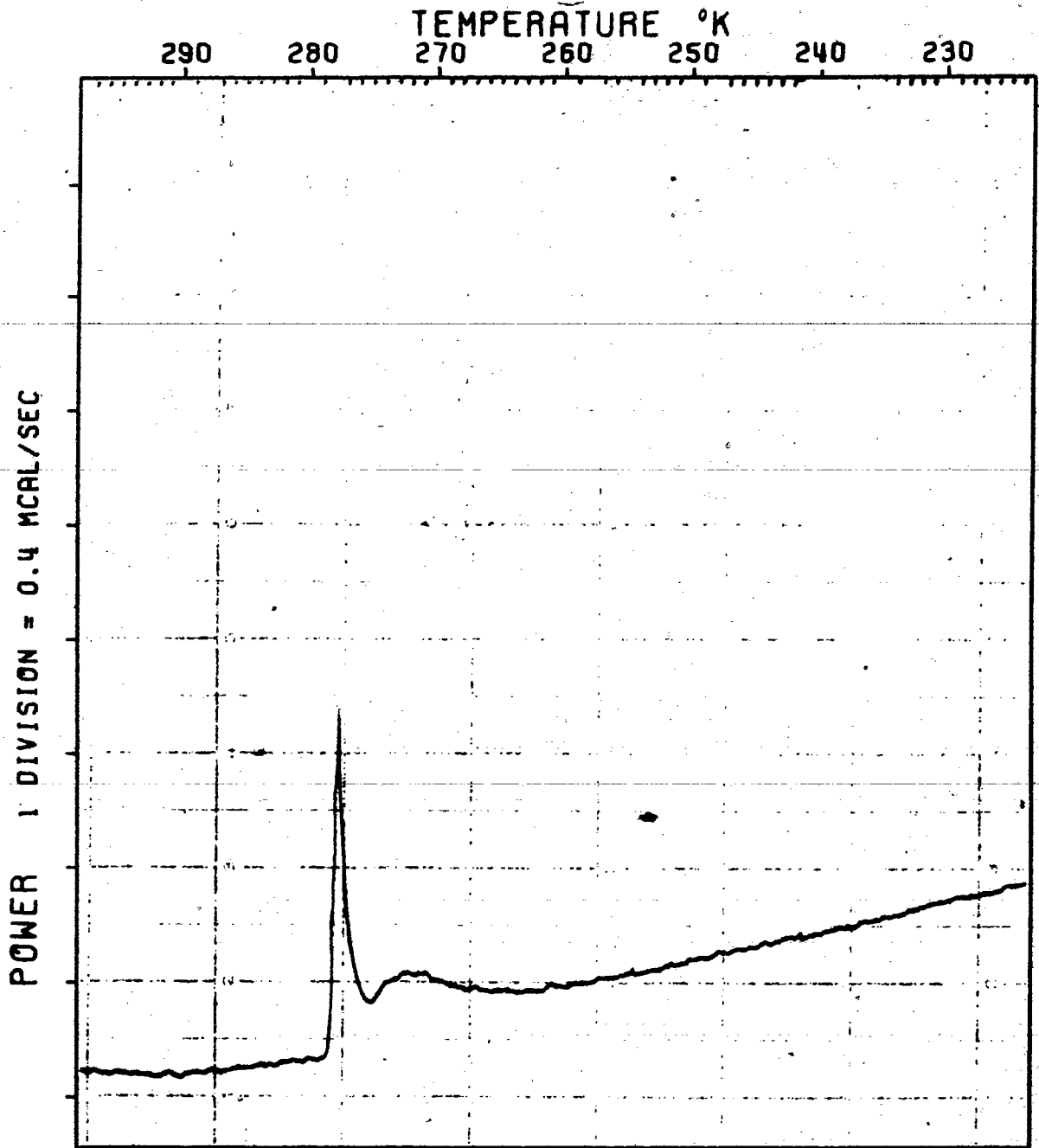


Fig. 25. DSC curve of the system benzene / charcoal 0.79 ± 0.03 g/g. Scan speed 2.5 °C/min. Range 0.4 mcal sec⁻¹ inch⁻¹.

equilibrium behaviour of the system.

The higher temperature peak in Fig. 22 - 25 is located at the same temperatures as the peak of pure benzene standard, and may be assigned to the melting of excessive unadsorbed benzene. The lower temperature peak, with the departure point from the relatively straight line at about 260 °K, can be assigned to the melting of the adsorbed benzene.

Quantitative estimation shows, that the total area of the peaks, between points $T=260$ °K and $T=283$ °K, represent only about 44% of the heat of fusion of the total benzene amounts in the samples. For the heat of fusion the normal melting point value 2.35 kcal/mol was taken (42). Comparison with NMR results (see Figures 3 and 6) shows rough agreement of the amounts of unfrozen benzene in the samples at 260 °K.

4.2.2. System benzene / silica gel

In Fig. 26 the curve A represents the DSC curve of the system benzene / silica gel 0.38 g/g. The curve B is the DSC curve of the blank run, without the adsorbent and adsorbate, shown for comparison because of nonlinearity of the calorimetric system in a broader temperature interval.

The position of the higher temperature peak suggests that it is caused by melting of the excessive unadsorbed benzene. The lower temperature peak may be assigned to the melting of the adsorbed benzene. Comparison with Figures 12 and 15 shows fair coincidence of the lower DSC peak temperature and the temperature region of maximum rate of change of C values.

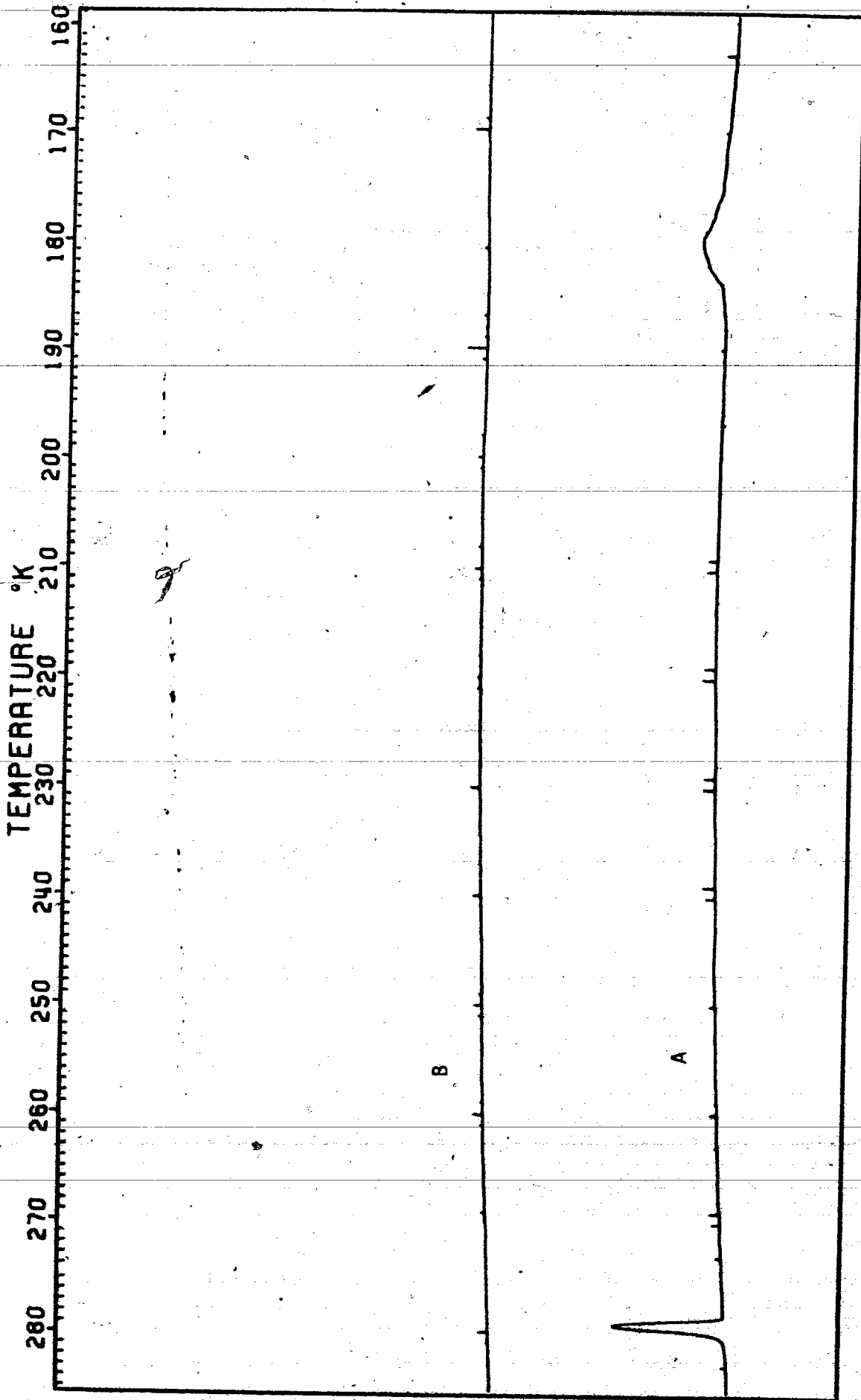


Fig. 26. A. DSC curve of the system benzene / silica gel 0.38 ± 0.01 g/g. Scan speed $10^\circ\text{C}/\text{min}$. Range $1.6 \text{ mcal sec}^{-1}\text{inch}^{-1}$.
B. Blank run; without adsorbent and adsorbate. Scan speed $10^\circ\text{C}/\text{min}$. Range $1.6 \text{ mcal sec}^{-1}\text{inch}^{-1}$.

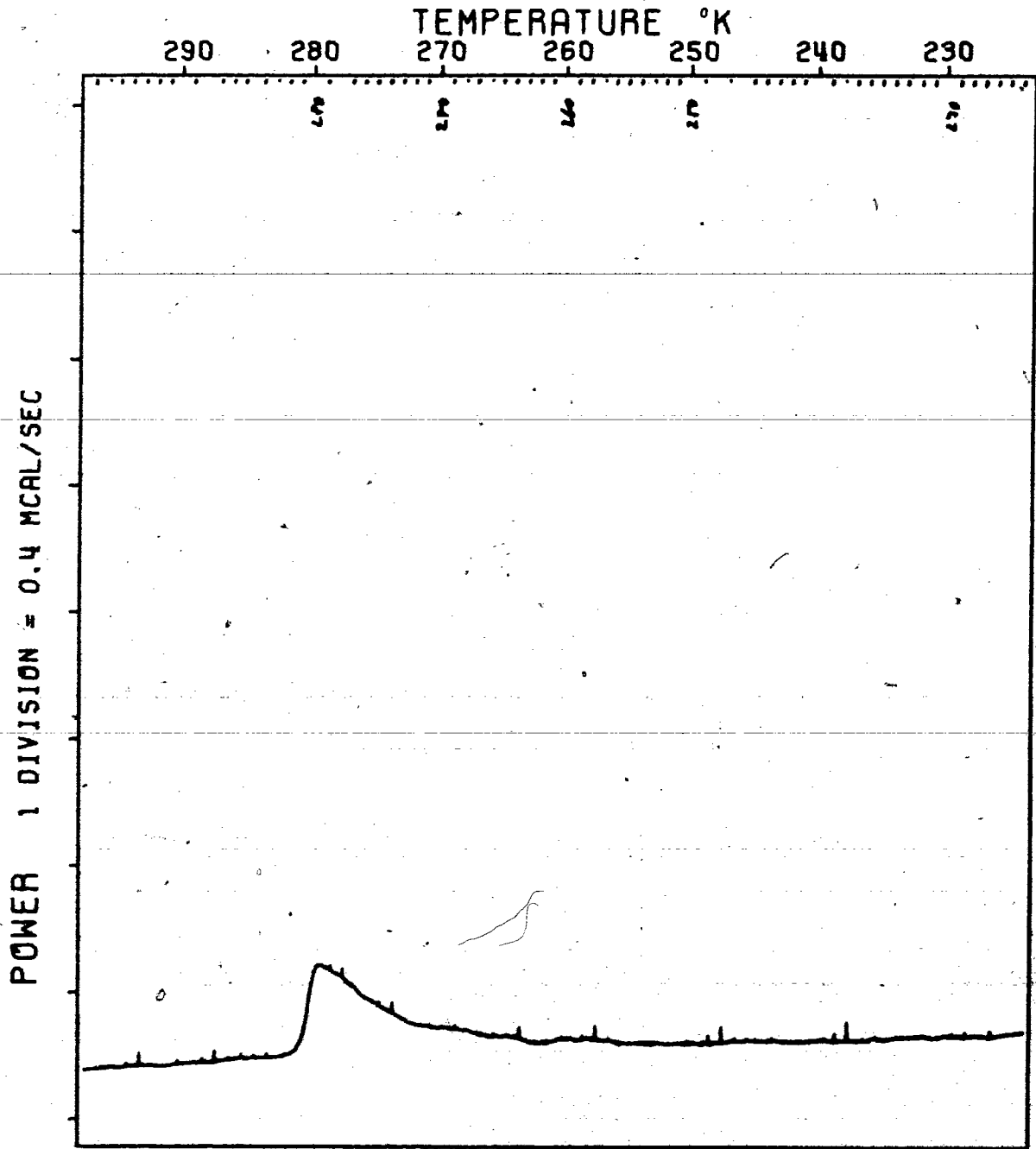


Fig. 27. DSC curve of the system benzene / cab-o-sil 0.39 + 0.002 g/g. Scan speed 10 °C/min. Range 0.4 mcal sec⁻¹ inch⁻¹.

From Figure 12 it follows, that the value of the limiting pore volume filling is about 0.26 g of benzene / g of silica gel. The excessive benzene amount in the DSC sample is then about 0.12 g/g. The quantitative estimation shows, that the amount of benzene calculated from the higher temperature peak area agrees well with that value. The area of the lower temperature peak represents about 80% of the adsorbed benzene, assuming that the heat of fusion of benzene is the same as at the normal melting point of bulk benzene.

4.2.3. System benzene / Cab-o-sil

The DSC curve of the sample 0.39 g of benzene / g of Cab-o-sil is shown in Figure 27. As can be seen, the departure of the curve from the straight line starts at 255 °K, that is well below the normal melting point of the bulk benzene.

5. Discussion

The NMR data for all three adsorption systems studied show that with decreasing temperature the NMR signal intensities and the corresponding values of C exhibit a sudden drop at some onset temperature and then they gradually decrease.

Comparison with DSC curves of the same adsorption systems shows that the temperatures at which those drops occur coincide fairly well with the temperatures of peaks on DSC curves. Also the temperature at which the departure from the relatively straight line occurs on the DSC curve coincide with the more significant change in the rate of change of C values.

The peaks on the DSC curves are assumed to be manifestations of first order phase transitions. Therefore it may be concluded that the NMR signal intensities and the corresponding values of C indicate changes in the content of the mobile phase during a first order phase transition, and that Resing's (34) theory of the apparent phase transition is not valid here.

Resing (34) has developed the theory, based on the Zimmerman and Brittin theory for relaxation in multiple phase systems (43), of an apparent-phase-transition effect due to a broad distribution of correlation times. The underlying principle is that if the system consists of two or more phases, characterized by different relaxation times, between which the physical exchange of the nuclei, characterized by a correlation time, is possible, then two limiting behaviors can occur. In the limit of fast exchange a single relaxation time is seen; in the limit of slow exchange each phase relaxes as if it were isolated

from all others. A phase is defined here in the NMR sense, as a group of nuclear spins having a given relaxation time.

For a system consisting of many phases and with a certain distribution of correlation times at a given temperature it might be expected that some of the phases would be effectively isolated at the slow exchange limit, some of the phases would be characterized by rapid exchange, and the remainder would be in the intermediate region. The proportions in the various regions of behavior would be expected to be a function of temperature. At high temperatures, characterized by faster molecular motions, all phases might be expected to exchange rapidly, while at low temperatures, where motion is slower, all phases might be effectively isolated. As the temperature of the system changes from sufficiently high temperature to a sufficiently low one a "phase transition" can be observed. However, there is no phase change in the thermodynamic sense of the term.

Resing (39) used an assumption of log-normal distribution of correlation times to fit NMR relaxation data for benzene adsorbed on charcoal with very good results. Unfortunately, no search for thermal effects was made, so it has not been proved if the behavior of the system is due to the "apparent phase transition" or the real thermodynamic phase transition. Our results on a similar system benzene / charcoal show the existence of a distinct thermal effect.

Of particular interest is the fact that the phase transition was detected on system benzene / cab-o-sil, because cab-o-sil can be considered as a nonporous adsorbent. This is in agreement with

Morrison's (7) observation, that the lowering of melting point of adsorbate is not restricted only to porous adsorbents.

Both NMR data and DSC measurements show that the phase transition in the adsorbed layer is not generally sharp process occurring at a single temperature, but that it proceeds, starting at some onset temperature, gradually with decreasing temperature.

These conclusions are in general agreement with the results of the NMR studies of similar systems such as water / silica gel by Barnes (23), benzene / silica gel by Woessner (38), benzene / charcoal by Thompson et al. (39), and the calorimetric studies of the systems n-hexane, benzene, and water adsorbed on silica gel (12), and benzene and carbon tetrachloride on silica gel (20). However, in the latter reference it is reported that no heat effect due to a phase transition has been found with the system benzene / charcoal.

Comparison of the behaviour of the systems benzene / Cab-o-sil and benzene / silica gel in the region of the phase transition shows features which may be attributed to the distinction between the adsorption on nonporous adsorbents and the adsorption on porous adsorbents in the region of the capillary condensation, where the adsorption can be correlated with the effective pore diameter or its distribution.

In the case of the system benzene / silica gel the detected onset temperature of freezing and the corresponding peak temperature on the DSC curve are quite distinct, the difference is about 80 °K, from the bulk freezing point even for the sample with completely filled capillaries and with excess bulk adsorbate.

In the case of the sample benzene / Cab-o-sil the onset temperature of freezing seems to increase with increasing adsorption and to approach the melting point of bulk adsorbate. As can be seen from Figure 27 the peaks on the DSC curve corresponding to the adsorbed and the excessive benzene coalesced.

That behaviour is compatible with the existing theories of the freezing of adsorbed substances.

For the porous adsorbents it is assumed that the liquid phase adsorbate is contained in capillaries of an effective radius r , and is in equilibrium with the adsorbate in the gaseous phase and with solid phase adsorbate present either as a bulk crystal or a solid contained in capillaries. By combining the Kelvin equation and the Clausius-Clapeyron equation a formula for the depression of the melting point of the adsorbate relative to the bulk melting point can be derived (40,5,19)

$$\ln T/T_0 = -2v_l \gamma_{l,g} / \Delta H_f r \quad (13)$$

or similarly for the solid phase adsorbate contained in capillaries and obeying the Kelvin equation (5,40,41)

$$\ln T/T_0 = 2(v_l \gamma_{l,g} - v_s \gamma_{s,g}) / \Delta H_f r \quad (14)$$

where T_0 is the phase transition temperature of the adsorbate in the capillary system, T is the triple point temperature of the bulk adsorbate, v_l and v_s are the molar volumes of the liquid and the solid respectively, ΔH_f is the molar heat of fusion, r is the radius of the capillary at the meniscus and $\gamma_{l,g}$ and $\gamma_{s,g}$ are the surface tensions of liquid and solid respectively.

An assumption involved in the derivation of the equations is that v_l , $\gamma_{l,g}$ and ΔH_f are constants, which may not be justified if the

depression of the melting point is large.

The equations (13 and (14) correlate the melting point depression with the pore diameter. The fact that the melting occurs over a range of temperatures can be explained by the distribution of values of the pore diameters in the adsorbent.

The value of r , calculated by means of equation (13) for $T=180$ °K using the values of ΔH_f , $\gamma_{l,g}$ and v_l at the normal melting point (namely 2.35 kcal/mol, 31.1 dyn/cm and 87.30 ml/mol), is 12.6 Å. A somewhat better approximation of r , using estimated* values of ΔH_f , $\gamma_{l,g}$ and v_l for the interval mean temperature 229 °K (2.18 kcal/mol, 36.2 dyn/cm and 82.73 ml/mol respectively), is 15.0 Å.

This value of r which corresponds to the peak value temperature on the DSC curve for the system benzene / silica gel is a reasonable expectation of the most frequent pore size for the type of silica gel used.

For the nonporous adsorbents it may be assumed that the whole available area of the adsorbent is covered with liquidlike adsorbate which is in equilibrium with the gas adsorbate and the solid adsorbate present as a bulk crystal. This model has been used by Patrick and Kemper (8), and Berezin and Kiselev (12). But as was pointed out by Morrison et al.(7), it implies that until the end of the melting process the adsorption isosteres must coincide with the sublimation curve in the P, T diagram which was not in agreement with their data on argon and nitrogen adsorbed on rutile.

* The value of v_l was estimated by means of Lydersen, Greenkorn and Hougen (44) correlation method, γ by using the nomograph by D.F. Othmer et al. (45), and ΔH_f by using of extrapolated c_p data taken from (46).

Another hypothesis in the case of nonporous adsorbent is that there can exist two distinct surface phases, one with molar entropy S_a^a , molar volume v_a^a and concentration Γ^a , the other with entropy S_a^b , molar volume v_a^b and concentration Γ^b (27,26, 7). The equation

$$RT(d \ln P/dT) = S_g - (\Gamma^a S_a^a - \Gamma^b S_a^b) / (\Gamma^a - \Gamma^b) \quad (15)$$

derived by Hill (27) for the equilibrium of the two surface phases and the gaseous phase defines a single line in a P,T diagram. It implies the existence of a single isostere in the melting region, which is not in agreement with experimental data, however, reconciliation can be achieved by considering surface heterogeneity (7).

Interesting and not quite clear is the origin of the cooling-reheating hysteresis in the temperature dependence of the NMR signal intensities and the corresponding C values observed on charcoal samples. Similar hysteresis was observed by Barnes (23) on the system water / silica, and by Morariu and Mills (37).

It seems that hysteresis involved may be of the type of super-cooled liquid hysteresis caused by nucleation kinetic factors, or of the type similar to adsorption - desorption hysteresis of porous adsorbents. However, it does not seem that hysteresis exhibited in Figures 1 - 6 is of the former type; the temperature dependence is gradual without any sudden changes. The latter type of hysteresis, which was suggested by Barnes, assumes that the adsorbate do not freeze in capillaries, but moves outside to form bulk solid. In this case it is not clear why the hysteresis was not observed also on the silica gel samples.

R E F E R E N C E S

- (1) Brunauer S., Adsorption of Gases and Vapors, Princeton University Press, Princeton 1945
- (2) Handbook of Applied Hydrology (V.T.Chow, ed.), McGraw Hill, New York 1964
- (3) Sidebottom E.W., Litvan G.G., Trans. Faraday Soc. 67, 2726 (1971)
- (4) Barnes G.T., Sanger R., Z. angew. Math. Phys. 12, 159 (1961)
- (5) Batchelor R.W., Foster A.G., Trans. Faraday Soc. 40, 300 (1944)
- (6) Brown M.J., Foster A.G., Nature 169, 37 (1952)
- (7) Morrison J.A., Drain L.E., Dugdale J.S., Can. J. Chem. 30, 890 (1952)
- (8) Patrick W.A., Kemper W.A., J. Phys. Chem. 42, 369 (1938)
- (9) Morrison J.A., Drain L.E., J. Chem. Phys. 19, 1063 (1951)
- (10) Dennis K.S., Pace E.L., Banghman C.S., J. Am. Chem. Soc. 75, 3269 (1953)
- (11) Siebert A.R., Pace E.L., J. Phys. Chem. 60, 828 (1956)
- (12) Berezin G.I. et al., J. Coll. Interface Sci. 45, 190 (1973)
- (13) Jones I.D., Gortner R.A., J. Phys. Chem. 36, 387 (1932)
- (14) Puri B.R., Sharma L.R., Lakhanpal M.L., J. Phys. Chem. 58, 289 (1954)
- (15) Hodgson C., McIntosh R., Can. J. Chem. 37, 1278 (1959)
- (16) Hodgson C., McIntosh R., Can. J. Chem. 38, 958 (1960)
- (17) Kipkie W.B., McIntosh R., Kelly B., J. Colloid and Interface Sci. 38, 3 (1972)
- (18) Higuti I., Sci. Rep. Tohoku Univ., Series I, 33, 174 (1949)
- (19) Higuti I., Shimizu M., J. Phys. Chem. 56, 198 (1952)
- (20) Higuti I., Iwagami Y., J. Phys. Chem. 56, 921 (1952)
- (21) Derouane E.G., Bull. Soc. Chim. Belges 78, 111 (1969)

- (22) Karagounis G. et al., Nature 221, 655 (1969)
- (23) Barnes G.T., Z. angew. Math. Phys. 13, 523 (1962)
- (24) Young D.M., Crowell A.D., Physical Adsorption of Gases, Butterworth, London 1962
- (25) Dubinin M.M. et al., Physical Adsorption at the Gas-Solid Interface, In Progress in Surface and Membrane Science (J.Danielli, ed.), p. 1, Academic Press, New York 1964
- (26) Meyer L., Long E., Phys. Rev. 85, 1035 (1952)
- (27) Hill T.L., J. Chem. Phys. 17, 520 (1949)
- (28) Hill T.L., J. Chem. Phys. 18, 246 (1950)
- (29) Brzhan V.S., Kristallografiya 4, 631 (1959)
- (30) Pople J.A., Schneider W.G., Bernstein H.J., High-resolution Nuclear Magnetic Resonance, McGraw Hill, New York 1959
- (31) Flockhart B.D., NMR and ESR Methods, in Comprehensive Analytical Chemistry (C.L.Wilson, ed.), Vol. 2c, Elsevier Publ. Co., Amsterdam 1971
- (32) Gutowsky H.S., Analytical Applications of NMR, In Physical Methods in Chemical Analysis (W.G.Berl, ed.), Vol. 3, p. 304, Academic Press, New York 1956
- (33) Williams R.B., Ann. N. Y. Acad. Sci., 70, 890 (1958)
- (34) Resing H.A., J. Chem. Phys. 43, 669 (1965)
- (35) Andrew E.R., Eades R.G., Proc. Roy. Soc. (London) A218, 537 (1953)
- (36) McClennan A.L., Harnsberger H.F., J. Colloid and Interface Sci. 23, 577 (1967)
- (37) Morariu V.V., Mills R., J. Colloid Interface Sci. 39, 406 (1972)
- (38) Wossner D.E., J. Phys. Chem. 70, 1217 (1966)
- (39) Thompson J.K., J. Chem. Phys. 43, 3853 (1965)
- (40) Kubelka P., Z. Elektrochem. 38, 611 (1932)
- (41) Morioka Y. et al., J. Colloid Interface Sci. 42, 156 (1973)
- (42) Beilsteins Handbuch der organischen Chemie, vierte Auflage, E III 5, 476, Springer - Verlag, Berlin 1972

- (43) Zimmerman J. R., Brittin W. E., J. Phys. Chem. 61, 1328 (1957)
- (44) Lydersen A. L. et al., Coll. Eng., Univ. Wisconsin,
Eng. Expt. Sta. Rept. 4, October 1955
- (45) Timmermans J., Physico - Chemical Constants, p.149,
Elsevier Publ. Co., New York 1950